AD649461

BRL R 1345

BRL

AD

REPORT NO. 1345

AERODYNAMIC AND FREQUENCY DEPENDENT ERRORS IN AN AIR BLAST GAGE

by

Henry J. Goodman

DDC
RELEASED
APR 5 1967
B

October 1966

Distribution of this document is unlimited.

U. S. ARMY MATERIEL COMMAND
BALLISTIC RESEARCH LABORATORIES
ABERDEEN PROVING GROUND, MARYLAND

ARCHIVE COPY

BALLISTIC RESEARCH LABORATORIES

REPORT NO. 1345

OCTOBER 1966

Distribution of this document is unlimited.

AERODYNAMIC AND FREQUENCY DEPENDENT ERRORS IN AN AIR BLAST GAGE

Henry J. Goodman

Terminal Ballistics Laboratory

RDT&E Project No. 1P014501A33E

ABERDEEN PROVING GROUND, MARYLAND

B A L L I S T I C R E S E A R C H L A B O R A T O R I E S

REPORT NO. 1345

HJGoodman/sjw
Aberdeen Proving Ground, Md.
October 1966

AERODYNAMICS AND FREQUENCY DEPENDENT ERRORS IN AN AIR BLAST GAGE

ABSTRACT

Tests were conducted in the Ballistic Research Laboratories (BRL) supersonic and hypersonic wind tunnel to determine the aerodynamic error due to mass flow around a pancake type gage. This air blast gage has been used extensively to measure the transient side-on pressure generated by an explosive charge. Data on flat surfaces are also presented.

The error due to mass flow is a function of both Mach number and Reynolds number. Error is largest near Mach one.

Measurements of impulse on gages with various shapes of pulses are considered. If there is no negative phase, impulse is independent of the gage size; the negative phase results in a low value of impulse for a gage longer than 1/10 the length of the positive phase.

TABLE OF CONTENTS

BLANK PAGE

LIST OF SYMBOLS

U = Shock front velocity (assumed constant across gage).

u = local mass velocity.

a = local sound velocity.

a_o = ambient sound velocity.

R = distance of shock front from center of charge along direction of shock propagation.

R_o = distance to center of gage from charge.

$R - R_o$ = s, distance from center of gage.

t = time, where $t = 0$ at $s = 0$.

t_o = $\frac{s}{U}$

s_o = radius of gage or half length of gage.

s_n = distance from center of gage to point on gage where pressure is measured.

ϕ = angle between axis and radius to gage element.

τ = thickness of gage.

L = width of gage.

W = weight of charge.

$\bar{t}$ = measured time to maximum negative pressure.

Δt = measured first positive duration.

$\Theta = \Theta_1$ = positive duration.

Θ_2 = constant.

$A(t_o)$ = area of gage covered by shock.

α = angle of attack.

M = $\frac{u_{fs}}{a_{fs}}$ free stream Mach number (flow Mach number when gage is not present).

P = ratio of excess pressure to excess pressure at the shock front.

p_1 = shock front pressure.

p_o = atmospheric pressure.

ρ = density of air.

q = $1/2\ \rho u^2$.

$I(s) = \int_{-\frac{s_o}{U}}^{\frac{s}{U}} P(s,t)\ dt$ impulse from shock front to time t.

Subscript

fs = free stream.

m = measured.

INTRODUCTION

The flow field behind a blast wave is disturbed when an object is placed in this field, and the disturbance created is dependent upon whether the mass flow is subsonic, transonic or supersonic. When the flow is subsonic a disturbance propagates with speed less than that of sound. Transonic flow consists of both subsonic and supersonic regions, whereas supersonic flow consists of a supersonic and subsonic region separated by a shock.

All of the above flow fields may occur when an air blast gage is placed in the flow field behind a blast wave to measure its pressure time profile. For weak shocks the waves may appear as in Figure 1. For strong shocks there may be an attached shock on the gage.

The present pancake gage is an improvement of the Ballistic Research Laboratories (BRL) Tourmaline gage which had an aspect ratio of approximately 4.0. This gage has a baffle configuration similar to that recommended by J. K. MacDonald and S. A. Schaaf.[1*] These men made theoretical computations on various plane forms and suggested the gage have a flat surface at the location of the transducer. Also in order to have an error of 5 percent or less the ratio of thickness to length ($\tau/2s_o$) should be kept less than 0.1. This gage, however, is found to disturb flow more than is tolerable when pressures are measured at reduced ambient pressures.

Tests were conducted in the BRL wind tunnel to determine the static pressure on the gage housing when subjected to supersonic mass flow. These measurements are for steady-state conditions and are not completely compatible with conditions that exist around a gage in an explosive blast field. The blast wave is transient; thus conditions behind the wave are unsteady. Impact effects due to the transmission of shocks through the mount are not considered in this discussion.

---

* *Superscript numbers denote references which may be found on page 64.*

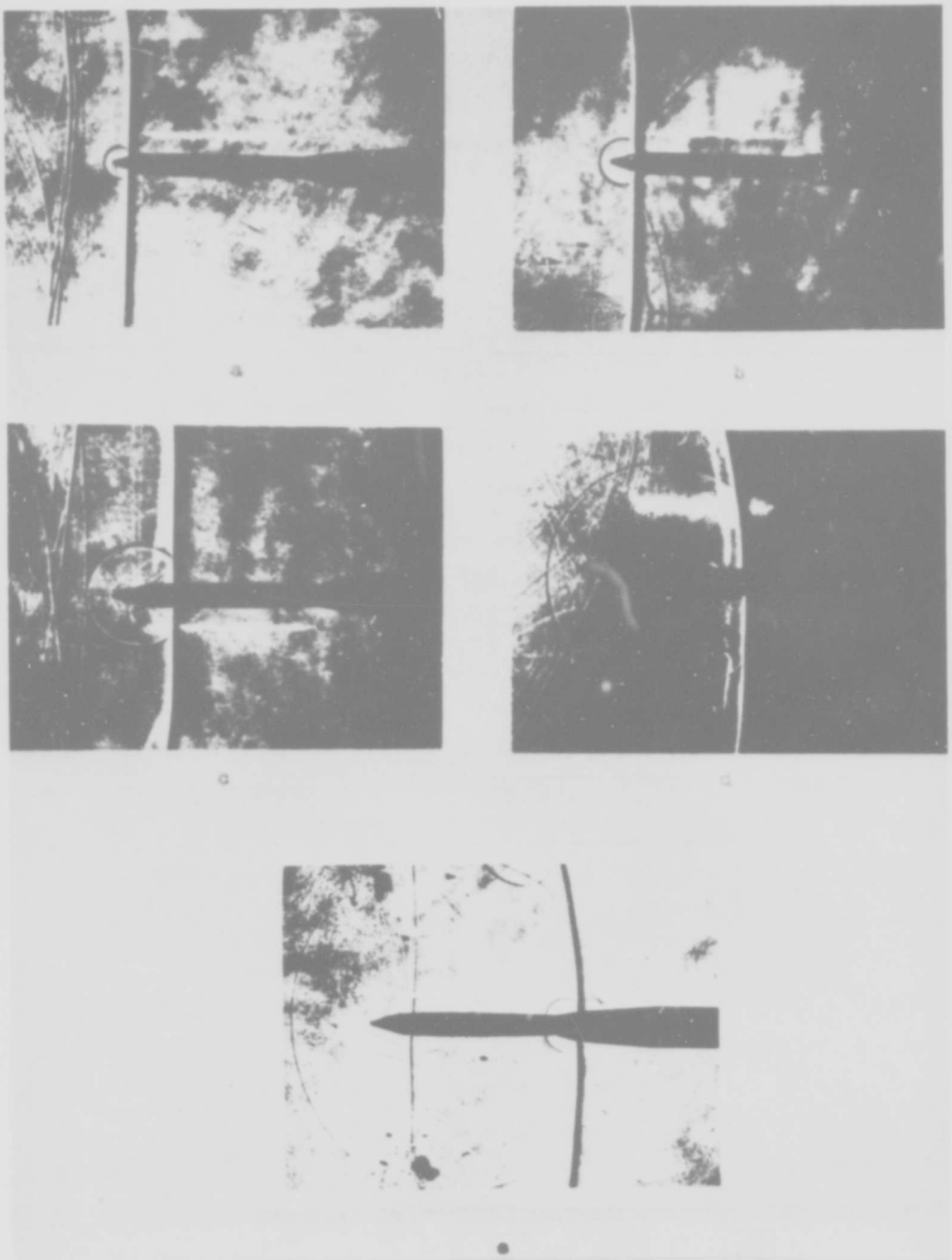

FIGURE 1 - WEAK TRANSIENT WAVE PROPAGATION OVER BRL PANCAKE GAGE

Flow conditions over test sections at subsonic and transonic flow are also considered since most blast pressure-time measurements are made in these flow ranges.

From the Hugoniot conditions one can show that the local flow velocity behind a plane shock in air is never greater than Mach 3.0 up to a shock pressure of 1000 atmospheres as shown in Table I. Thus the blast gage never experiences local mass flow velocities greater than Mach 3.0 when subject to blast from Pentolite or a comparable explosive. The flow velocity u for a blast wave corresponds to the flow velocity u_{fs} in the wind tunnel. The measurements of pressures in either the field behind the blast wave or the test section of the wind tunnel must not be made at flow velocities where the ratio $\frac{u}{a} = \frac{u_{fs}}{a_{fs}} = 1$. However, in the case of transient blast waves, velocity ratio $\frac{u}{a}$ does pass through 1 when pressure ratios greater than 4.82 are encountered.

In addition to the experimental study of steady flow, the response of the gage element to triangular and Friedlander pressure pulses is considered.

EXPERIMENTAL SETUP

A two-inch model of the BRL side-on blast gage was constructed according to specifications shown in Figure 2. These specifications were prepared by CPT E. J. Staros previously of the Special Problems Branch of the Terminal Ballistics Laboratory (TBL). The gage was mounted to a support adaptable to both the supersonic and hypersonic wind tunnels of BRL. Figure 3 shows the gage orientation in the test chamber. Pictures a and b show the initial configuration while c and d show the gage with a flat plate attached, and e shows the gage with a needle attached. A modified gage which had been sand blasted to roughen the surface was also used.

TABLE I

Properties of Air Along the Hugoniot Curve

P_1/p_o	U/a_o	u/a
1.25	1.10	.157
1.35	1.14	.210
1.50	1.20	.282
1.55	1.21	.304
1.80	1.30	.403
2.05	1.38	.488
2.10	1.39	.504
2.45	1.50	.602
2.90	1.61	.707
3.40	1.75	.802
3.90	1.87	.882
4.00	1.89	.896
4.10	1.91	.910
4.40	1.98	.950
5.50	2.20	1.08
7.16	2.50	1.22
8.00	2.64	1.27
14.3	3.50	1.54
23.9	4.50	1.75
42.2	5.93	1.97
42.6	5.96	1.97
67.4	7.44	2.18
67.9	7.47	2.18
650	22.5	3.00
900	26.4	3.02
1000	27.9	3.00

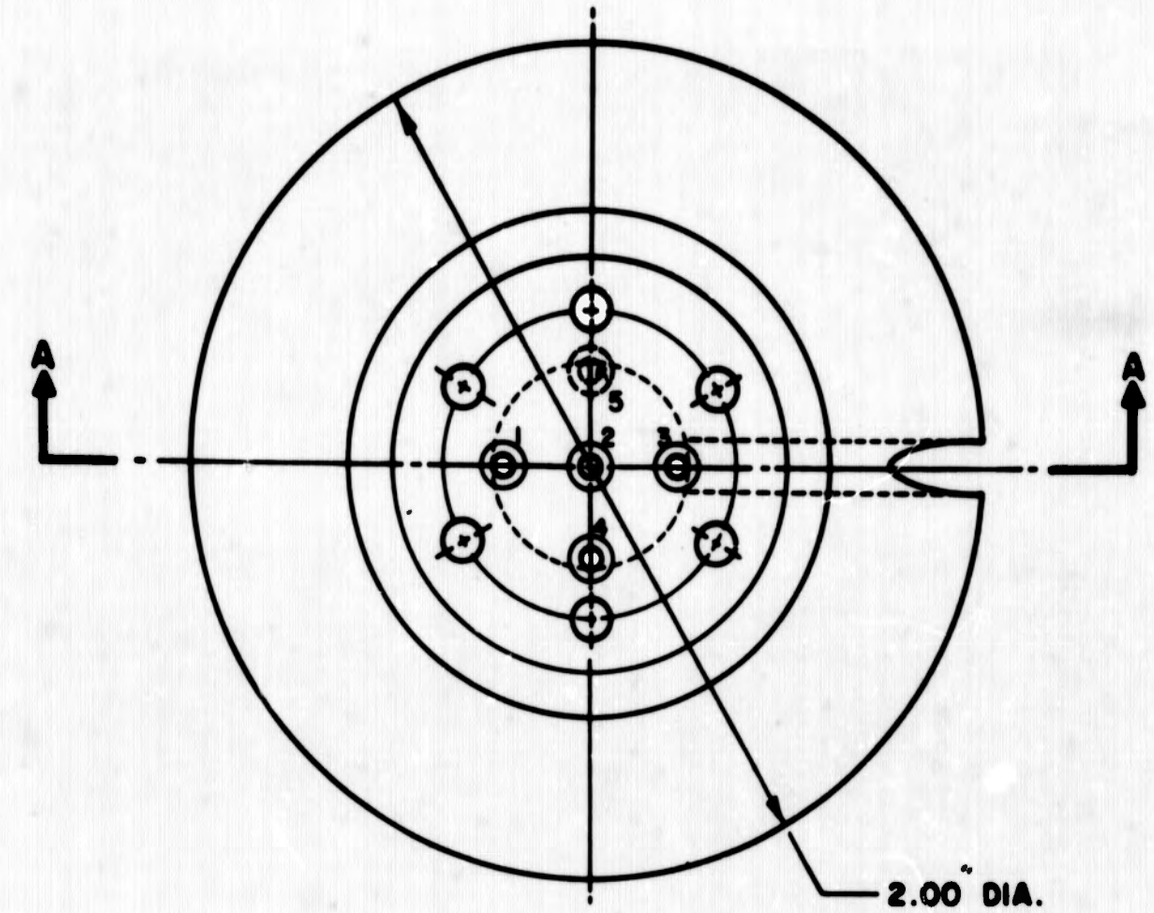

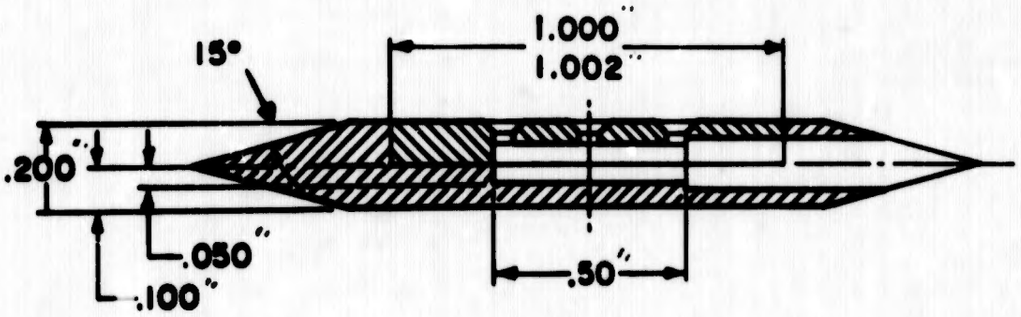

SECTION A-A

FIOURE 2 - SCALED DRAWING OF TWO INCH PANCAKE GAGE.

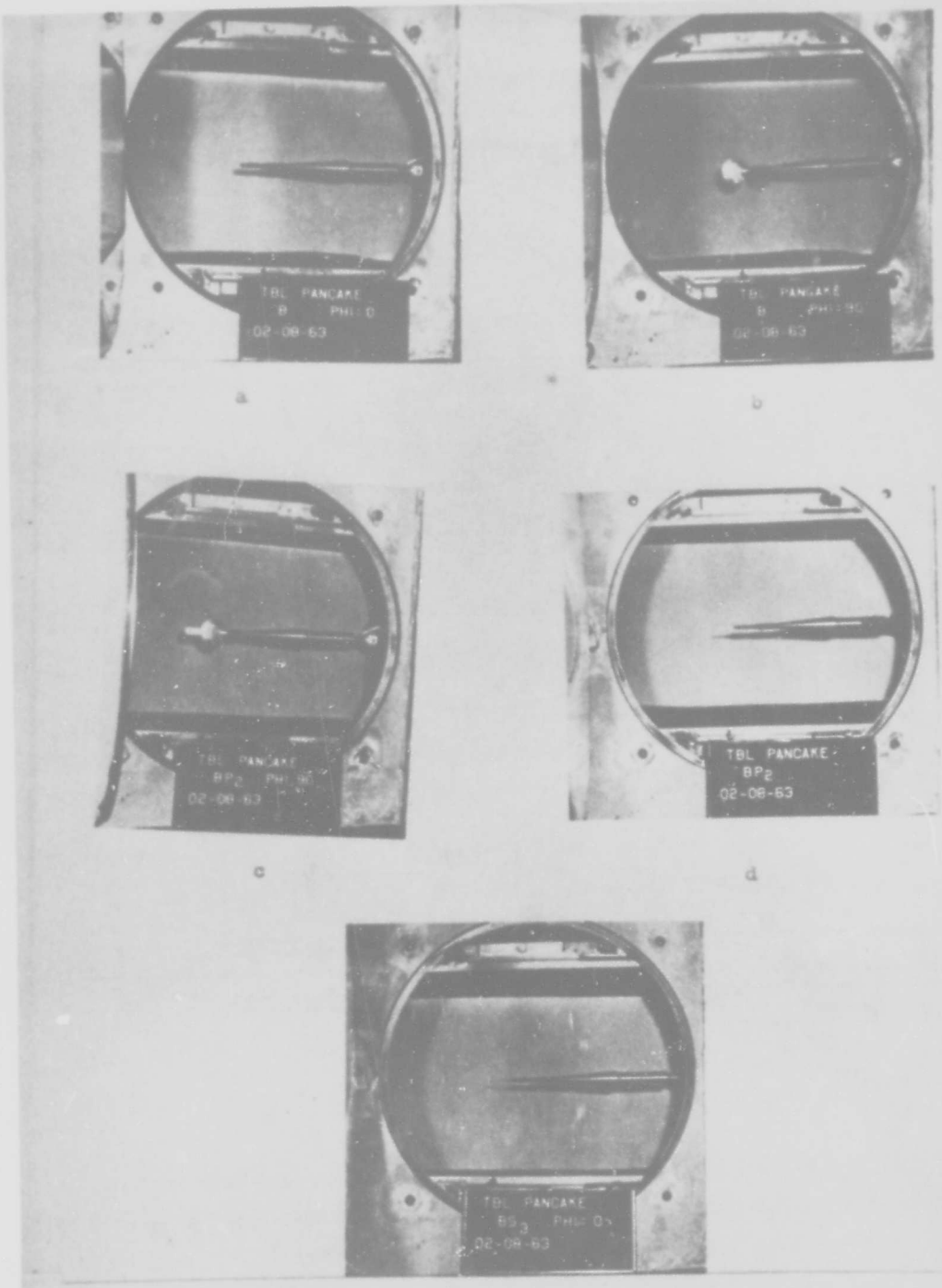

FIGURE 3 - WIND TUNNEL MOUNTING OF SEVERAL CONFIGURATIONS OF BRL PANCAKE GAGE.

Five orifices were placed in the gage housing as shown in Figure 2. Four orifices were placed on one side of the gage and one on the other side. Table II gives the position of the orifice and thickness ratio $(s_n + s_o)/\tau$ of the gage. The value $s_n + s_o$ is the distance from the leading edge of the measuring device to the point where pressure is measured.

A series of tests were run at Mach 1.75 through Mach 7 at angles of attack from 0 to 5 degrees. The Reynolds number* was varied at the different Mach numbers by changing the stagnation pressure. These data are in Table III. The pressure indicated by (2 + 4 + 5)/3 is the average pressure at the middle of the gage. Orifice 5 was on one side of the gage and orifices 1, 2, 3 and 4 were on the other side. Thus, orifices 4 and 5 show the edge effect and effect due to angle of attack. Orifices 1, 2 and 3 show the leading edge effect. The pressure value indicated by (2 + 4 + 5)/3 shows the averaging effect reduces error due to angle of attack. In the velocity range of interest the error due to angle of attack greater than 1 degree is larger than 10 percent. Error due to edge effect is negligible.

All tests conducted on the modified gage were at Mach 4.5 and zero angle of attack. These data are presented in Table IV. These measurements on the modified gage along with the original measurements have values that are consistently high when a smooth curve is drawn through all the measured values; therefore, these data are considered separately.

Table V shows modifications of the gage and Figures 4 and 5 are schlieren photographs of the flow at Mach 4.5 over the modified gage. The photographs (1-13) in Figures 4 and 5 correspond to configurations (1-13) respectively in Table V.

---

* *Reynolds number* $RE = \frac{\rho u L}{\nu}$ *where L is some characteristic length of the model and* ν *is the coefficient of viscosity of the fluid.*

TABLE II

Position of Taps on Gage

Orifice No.	Distance Inches $s_n + s_o$	Thickness Inches τ	$\left(\frac{\text{Distance}}{\text{Thickness}}\right)$ $(s_n + s_o)/\tau$
1	.796	.20	3.98
2	1.000	.20	5.00
3	1.204	.20	6.02
4	1.000	.20	5.00
5	1.000	.20	5.00

TABLE III

Pressure on Side-On Blast Gage When Placed in Supersonic Wind Tunnel

M = 1.75, RE = 0.24 x 10^6/in, p_o = 0.712 atm, q = 0.28 atm

α degree	p_{fs} atm	p_m/p_{fs} Orifice #					
		1	2	3	4	5	(2+4+5)/3
0	.134	.933	.936	.946	.931	.938	.935
0	.135	.928	.931	.941	.926	.931	.929
1	.135	.968	.969	.978	.964	.894	.966
-1	.135	.890	.894	.906	.888	.971	.891
3	.135	1.053	1.052	1.059	1.046	.825	1.045
5	.135	1.132	1.133	1.140	1.128	.759	1.130

M = 1.75, RE = 0.48 x 10^6/in, p_o = 1.42 atm, q = 0.573 atm

α degree	p_{fs} atm	p_m/p_{fs} Orifice #					
		1	2	3	4	5	(2+4+5)/3
0	.268	.915	.920	.930	.910	.921	.917
0	.268	.916	.920	.932	.911	.921	.917
1	.268	.954	.958	.969	.949	.883	.954
-1	.268	.876	.882	.895	.874	.961	.878
3	.268	1.038	1.038	1.047	1.030	.811	1.034

M = 2.50, RE = 0.24 x 10^6/in, p_o = 0.994 atm, q = 0.256 atm

α degree	p_{fs} atm	p_m/p_{fs} Orifice #					
		1	2	3	4	5	(2+4+5)/3
0	.0592	.966	.957	.962	.952	.962	.957
0	.0592	.969	.959	.967	.955	.962	.959
1	.0592	1.028	1.017	1.026	1.014	.905	1.016
-1	.0593	.911	.905	.912	.901	1.021	.903
3	.0592	1.159	1.147	1.146	1.141	.800	1.144
5	.0592	1.294	1.281	1.284	1.274	.706	1.275

TABLE III (Contd)

Pressure on Side-On Blast Gage When Placed in Supersonic Wind Tunnel

M = 2.50, RE = 0.48 x 10^6/in, p_o = 2.13 atm, q = 0.513 atm

α degree	p_{fs} atm	p_m/p_{fs} Orifice # 1	2	3	4	5	(2+4+5)/3
0	.126	.947	.942	.951	.934	.951	.942
0	.126	.950	.942	.953	.936	.951	.943
1	.126	1.012	1.005	.1015	.997	.894	1.001
-1	.126	.893	.886	.896	.880	1.011	.883
3	.126	1.142	1.134	1.142	1.124	.788	1.129

M = 3.50, RE = 0.24 x 10^6/in, p_o = 1.65 atm, q = 0.186 atm

α degree	p_{fs} atm	p_m/p_{fs} Orifice # 1	2	3	4	5	(2+4+5)/3
0	.0218	1.016	1.009	.981	.988	.997	.998
0	.0213	1.051	1.022	1.019	1.019	1.019	1.020
1	.0214	1.137	1.102	1.102	1.105	.936	1.104
-1	.0214	.981	.949	.946	.946	1.096	.948
3	.0213	1.319	1.291	1.249	1.291	.799	1.291
5	.0213	1.527	1.495	1.489	1.492	.703	1.494

M = 3.50, RE = 0.48 x 10^6/in, p_o = 3.30 atm, q = 0.372 atm

α degree	p_{fs} atm	p_m/p_{fs} Orifice # 1	2	3	4	5	(2+4+5)/3
0	.0429	1.006	.981	.981	.979	.994	.985
0	.0430	1.013	.986	.987	.984	.994	.988
1	.0430	1.095	1.071	1.070	1.066	.913	1.016
-1	.0432	.938	.911	.911	.910	1.078	.943
3	.0429	1.285	1.262	1.262	1.257	.769	1.096
5	.0428	1.503	1.478	1.475	1.471	.654	1.201

TABLE III (Contd)

Pressure on Side-On Blast Gage When Placed in Supersonic Wind Tunnel

M = 4.5, RE = 0.24 x 10^6/in, p_o = 2.58 atm, q = 0.127 atm

α degree	p_{fs} atm	p_m/p_{fs} Orifice #					
		1	2	3	4	5	(2+4+5)/3
0	.00871	1.242	1.172	1.164	1.188	1.188	1.183
0	.00864	1.331	1.260	1.260	1.276	1.181	1.239
1	.00871	1.422	1.352	1.344	1.367	1.070	1.268
-1	.00871	1.234	1.172	1.203	1.203	1.273	1.188
3	.00871	1.648	1.578	1.562	1.586	.914	1.582
5	.00864	1.874	1.811	1.780	1.811	.835	1.811

M = 4.5, RE = 0.48 x 10^6/in, p_o = 5.18 atm, q = 0.254 atm

α degree	p_{fs} atm	p_m/p_{fs} Orifice #					
		1	2	3	4	5	(2+4+5)/3
0	.0178	1.138	1.077	1.061	1.080	1.023	1.060
0	.0178	1.207	1.149	1.130	1.146	1.046	1.114
1	.0182	1.270	1.210	1.195	1.210	.948	1.123
-1	.0178	1.084	1.031	1.004	1.031	1.184	1.082
3	.0177	1.512	1.442	1.438	1.450	.823	1.238
5	.0177	1.781	1.731	1.715	1.727	.788	1.415

TABLE III (Contd)

Pressure on Side-On Blast Gage When Placed in Supersonic Wind Tunnel

M = 5.93, RE = 0.24 x 10^6/in, p_o = 14.5 atm, q = 0.243 atm

α degree	p_{fs} atm	p_m/p_{fs} Orifice #					
		1	2	3	4	5	(2+4+5)/3
0	.01	1.461	1.328	1.261	1.323	1.318	1.323
0	.01	1.446	1.323	1.248	1.306	1.306	1.312
1	.01	1.601	1.473	1.398	1.448	1.196	1.460
-1	.01	1.315	1.198	1.123	1.180	1.425	1.189
3	.01	1.861	1.808	1.743	1.798	1.005	1.803
-3	.01	1.093	.9880	.9129	.9655	1.791	.9768
5	.01	2.321	2.210	2.148	2.211	.860	2.211

M = 5.96, RE = 0.48 x 10^6/in, p_o = 289.8 atm, q = 0.476 atm

α degree	p_{fs} atm	p_m/p_{fs} Orifice #					
		1	2	3	4	5	(2+4+5)/3
0	.02	1.376	1.243	1.182	1.247	1.234	1.242
0	.02	1.384	1.251	1.193	1.254	1.248	1.251
1	.02	1.531	1.404	1.345	1.395	1.120	1.400
-1	.02	1.253	1.129	1.067	1.132	1.390	1.130
3	.02	1.866	1.748	1.698	1.746	.9241	1.747
-3	.02	1.039	.9151	.8492	.9151	1.725	.9151

M = 6.00, RE = 0.72 x 10^6/in, p_o = 43.47 atm, q = 0.694 atm

α degree	p_{fs} atm	p_m/p_{fs} Orifice #					
		1	2	3	4	5	(2+4+5)/3
0	.03	1.378	1.256	1.199	1.253	1.243	1.251
0	.03	1.369	1.246	1.187	1.241	1.506	1.244
1	.03	1.522	1.399	1.347	1.395	1.104	1.397
-1	.03	1.243	1.111	1.053	1.113	1.379	1.112
3	.03	1.878	1.766	1.721	1.752	.8865	1.759
-3	.03	1.020	.8964	.8346	.8937	1.743	.8950

TABLE III (Contd)

Pressure on Side-On Blast Gage When Placed in Supersonic Wind Tunnel

M = 7.42, RE = 0.12 x 10^6/in, p_o = 16.33 atm, q = 0.105 atm

α degree	p_{fs} atm	p_m/p_{fs} Orifice # 1	2	3	4	5	(2+4+5)/3
0	.0029	2.348	2.294	2.131	2.212	2.194	2.233
3	.0029	2.956	2.774	2.602	2.738	2.058	2.756
-3	.0029	1.931	1.922	1.795	1.877	2.602	1.900

M = 7.44, RE = 0.24 x 10^6/in, p_o = 32.65 atm, q = 0.2068 atm

α degree	p_{fs} atm	p_m/p_{fs} Orifice # 1	2	3	4	5	(2+4+5)/3
0	.0058	2.052	1.873	1.754	1.818	1.841	1.844
0	.0058	2.002	1.666	1.689	1.795	1.772	1.744
1	.0058	2.222	2.025	1.887	1.988	1.680	2.006
-1	.0058	1.841	1.680	1.547	1.634	1.910	1.657
3	.0058	2.708	2.497	2.337	2.447	1.492	2.472
-3	.0058	1.561	1.432	1.313	1.391	2.378	1.412
-5	.0058	1.327	1.244	1.157	1.203	2.966	1.222

M = 7.47, RE = 0.48 x 10^6/in, p_o = 65.31 atm, q = 0.407 atm

α degree	p_{fs} atm	p_m/p_{fs} Orifice # 1	2	3	4	5	(2+4+5)/3
0	.011	1.825	1.607	1.486	1.595	1.579	1.560
3	.011	2.477	2.259	2.140	2.245	1.173	2.252
-3	.011	1.380	1.183	1.067	1.157	2.200	1.170

TABLE IV

Pressure on Side-On Blast Gage When Placed in Supersonic Wind Tunnel

CONFIGURATION B MODIFIED

M = 4.5, RE = 0.48 x 10^6/in, p_o = 5.22 atm, q = 0.254 atm

α degree	p_{fs} atm	p_m/p_{fs} Orifice # 1	2	3	4	5	(2+4+5)/3
0	.0179	1.262	1.122	1.068	1.114	1.110	1.115

CONFIGURATION B MODIFIED

M = 4.5, RE = 0.24 x 10^6/in, p_o = 26.1 atm, q = 0.127 atm

α degree	p_{fs} atm	p_m/p_{fs} Orifice # 1	2	3	4	5	(2+4+5)/3
0	.0088	1.349	1.233	1.194	1.209	1.209	1.217

CONFIGURATION B MODIFIED

M = 4.5, RE = 0.48 x 10^6/in, p_o = 5.22 atm, q = 0.254 atm

α degree	p_{fs} atm	p_m/p_{fs} Orifice # 1	2	3	4	5	(2+4+5)/3
0	.0150	1.117	1.072	1.057	1.076	1.083	1.077

CONFIGURATION B* MODIFIED

M = 4.5, RE = 0.24 x 10^6/in, p_o = 2.61 atm, q = 0.127 atm

α degree	p_{fs} atm	p_m/p_{fs} Orifice # 1	2	3	4	5	(2+4+5)/3
0		1.177	1.115	1.100	1.123	1.123	1.120

* *Model has all stainless steel tubing.*

TABLE IV (Contd)

Pressure on Side-On Blast Gage When Placed in Supersonic Wind Tunnel

CONFIGURATION B

M = 4.5, RE = 0.48 x 10^6/in, p_o = 5.22 atm, q = 0.254 atm

α degree	p_{fs} atm	p_m/p_{fs} Orifice #					
		1	2	3	4	5	(2+4+5)/3
0	.0182	1.120	1.049	1.034	1.056	-	1.052
0	.0179	1.137	1.068	1.049	1.072	-	1.070
0	.0180	1.129	1.057	1.042	1.068	-	1.062
0	.0178	1.134	1.084	1.061	1.073	1.088	1.082
1	.0179	1.236	1.167	1.156	1.179	-	1.178
-1	.0179	1.042	.973	.951	.989	-	.981
2	.0180	1.347	1.279	1.268	1.298	-	1.289
-2	.0180	.958	.890	.864	.898	-	.894
3	.01412	1.470	1.398	1.398	1.425	-	1.411

CONFIGURATION B

M = 4.5, RE = 0.24 x 10^6/in, p_o = 2.61 atm, q = 0.127 atm

α degree	p_{fs} atm	p_m/p_{fs} Orifice #					
		1	2	3	4	5	(2+4+5)/3
0	.0087	1.289	1.219	1.195	1.203	-	1.21
0	.0088	1.246	1.177	1.154	1.177	-	1.177
0	.0088	1.208	1.131	1.123	1.138	-	1.135
0	.0087	1.227	1.219	1.180	1.180	1.180	1.193
1	.0088	1.338	1.277	1.246	1.300	-	1.288
-1	.0088	1.177	1.108	1.077	1.123	-	1.116
2	.0088	1.450	1.380	1.357	1.372	-	1.376
-2	.0088	1.100	1.038	1.000	1.031	-	1.035
3	.0087	1.563	1.492	1.469	1.492	-	1.492
-3	.0088	1.038	.977	.938	.969	-	.973

TABLE IV (Contd)

Pressure on Side-On Blast Gage When Placed in Supersonic Wind Tunnel

CONFIGURATION BS 1

M = 4.5, RE = 0.48 x 10^6/in, p_o = 5.22 atm, q = 0.254 atm

α degree	p_{fs} atm	p_m/p_{fs} Orifice # 1	2	3	4	5	(2+4+5)/3
0	.0180	1.159	1.038	1.015	1.080	-	1.059
0	.0181	1.143	1.030	1.004	1.068	-	1.049
0	.0180	1.167	1.057	1.030	1.084	-	1.080
-.5	.0182	1.094	.981	.959	1.015	-	.998

CONFIGURATION BS 1

M = 4.5, RE = 0.24 x 10^6/in, p_o = 2.61 atm, q = 0.127 atm

α degree	p_{fs} atm	p_m/p_{fs} Orifice # 1	2	3	4	5	(2+4+5)/3
0	.0087	1.227	1.125	1.094	1.156	-	1.140
0	.0088	1.194	1.085	1.062	1.124	-	1.104
0		1.256	1.163	1.132	1.140	1.155	1.153

CONFIGURATION BS 2

M = 4.5, RE = 0.48 x 10^6/in, p_o = 5.22 atm, q = 0.25 atm

α degree	p_{fs} atm	p_m/p_{fs} Orifice # 1	2	3	4	5	(2+4+5)/3
0	.0181	1.244	1.073	.996	1.060	-	1.068
0	.0181	1.229	1.068	1.011	1.064	-	1.066
0	.0179	1.247	1.091	1.027	1.080	-	1.086
0	.0178	1.257	1.107	1.034	1.092	1.069	1.089
.5	.0181	1.244	1.090	1.053	1.113	-	1.102
-.5	.0181	1.199	1.043	.985	1.008	-	1.026

TABLE IV (Contd)

Pressure on Side-On Blast Gage When Placed in Supersonic Wind Tunnel

CONFIGURATION BS 2

M = 4.5, RE = 0.24 x 10^6/in, p_o = 2.61 atm, q = 0.127 atm

α degree	p_{fs} atm	p_m/p_{fs} Orifice #					
		1	2	3	4	5	(2+4+5)/3
0	.0087	1.359	1.156	1.094	1.148	-	1.132
0	.0088	1.315	1.138	1.069	1.131	-	1.135
0	.0087	1.344	1.094	1.094	1.141	-	1.118

CONFIGURATION BS 3

M = 4.5, RE = 0.48 x 10^6/in, p_o = 5.2 atm, q = 0.254 atm

α degree	p_{fs} atm	p_m/p_{fs} Orifice #					
		1	2	3	4	5	(2+4+5)/3
0	.0180	1.280	1.117	1.057	1.068	-	1.093
0	.0180	1.279	1.117	1.053	1.064	-	1.090
0	.0180	1.268	1.102	1.042	1.068	-	1.085
1	.0180	1.302	1.158	1.117	1.177	-	1.168
-1	.0180	1.192	1.057	.996	.981	-	1.019
3	.0180	1.392	1.370	1.404	1.434	-	1.402
-3	.0180	.962	.853	.811	.819	-	.836

CONFIGURATION BS 3

M = 4.5, RE = 0.24 x 10^6/in, p_o = 2.61 atm, q = 0.127 atm

α degree	p_{fs} atm	p_m/p_{fs} Orifice #					
		1	2	3	4	5	(2+4+5)/3
0	.0087	1.438	1.227	1.148	1.141	-	1.184
0	.0088	1.423	1.231	1.146	1.169	-	1.200
0	.0088	1.408	1.192	1.116	1.108	-	1.150
1	.0088	1.446	1.262	1.208	1.269	-	1.266
-1	.0088	1.408	1.185	1.092	1.100	-	1.143
3	.0088	1.488	1.403	1.426	1.442	-	1.423
-3	.0088	1.177	1.185	.977	.985	-	1.085

TABLE IV (Contd)

Pressure on Side-On Blast Gage When Placed in Supersonic Wind Tunnel

CONFIGURATION BS 4

M = 4.5, RE = 0.48 x 10^6/in, p_o = 5.2 atm, q = 0.254 atm

α degree	p_{fs} atm	p_m/p_{fs} Orifice # 1	2	3	4	5	(2+4+5)/3
0	.0181	1.248	1.117	1.064	1.079	-	1.098
0	.0181	1.253	1.121	1.068	1.087	-	1.104
0	.0181	1.241	1.105	1.064	1.075	-	1.090
0	.0181	1.285	1.131	1.065	1.085	1.085	1.100
1	.0181	1.309	1.174	1.140	1.192	-	1.183
-1	.0181	1.158	1.038	.989	.974	-	1.006
2	.0181	1.331	1.237	1.259	1.289	-	1.263
-2	.0181	1.053	.929	.887	.914	-	.922
3	.0181	1.398	1.372	1.410	1.417	-	1.394
-3	.0181	.974	.842	.801	.846	-	.844

CONFIGURATION BS 4

M = 4.5, RE = 0.24 x 10^6/in, p_o = 2.61 atm, q = 0.127 atm

α degree	p_{fs} atm	p_m/p_{fs} Orifice # 1	2	3	4	5	(2+4+5)/3
0	.0087	1.328	1.234	1.180	1.156	-	1.195
0	.0088	1.134	1.256	1.217	1.178	-	1.217
0	.0089	1.290	1.191	1.145	1.115	-	1.153
0	.0087	1.375	1.273	1.203	1.180	1.148	1.200
1	.0088	1.403	1.295	1.248	1.256	-	1.276
-1	.0088	1.295	1.209	1.147	1.140	-	1.174
3	.0087	1.500	1.422	1.453	1.477	-	1.450
-3	.0088	1.186	1.054	1.163	1.031	-	1.042

TABLE IV (Contd)

Pressure on Side-On Blast Gage When Placed in Supersonic Wind Tunnel

CONFIGURATION BS 4* MODIFIED

M = 4.5, RE = 0.48 x 10^6/in, p_o = 5.2 atm, q = 0.254 atm

α degree	p_{fs} atm	p_m/p_{fs} Orifice # 1	2	3	4	5	(2+4+5)/3
0	.0178	1.244	1.137	1.076	1.084	1.076	1.10

CONFIGURATION BS 4* MODIFIED

M = 4.5, RE = 0.24 x 10^6/in, p_o = 2.41 atm, q = 0.127 atm

α degree	p_{fs} atm	p_m/p_{fs} Orifice # 1	2	3	4	5	(2+4+5)/3
0	.0088	1.318	1.233	1.155	1.132	1.116	1.160

CONFIGURATION BP_1 MODIFIED

M = 4.5, RE = 0.48 x 10^6/in, p_o = 5.2 atm, q = 0.254 atm

α degree	p_{fs} atm	p_m/p_{fs} Orifice # 1	2	3	4	5	(2+4+5)/3
0	.0180	1.068	1.083	1.083	1.091	1.091	1.088

CONFIGURATION BP_1 MODIFIED

M = 4.5, RE = 0.24 x 10^6/in, p_o = 2.61 atm, q = 0.127 atm

α degree	p_{fs} atm	p_m/p_{fs} Orifice # 1	2	3	4	5	(2+4+5)/3
0	.0086	1.206	1.183	1.167	1.183	1.183	1.178

* *Model has all stainless steel tubing.*

TABLE IV (Contd)

Pressure on Side-On Blast Gage When Placed in Supersonic Wind Tunnel

CONFIGURATION BP_2

M = 4.5, RE = 0.48 x 10^6/in, p_o = 5.2 atm, q = 0.254 atm

α degree	p_{fs} atm	p_m/p_{fs} Orifice # 1	2	3	4	5	(2+4+5)/3
0	.0178	1.095	1.118	1.115	1.088	1.061	1.089

CONFIGURATION BP_2

M = 4.5, RE = 0.24 x 10^6/in, p_o = 2.61 atm, q = 0.127 atm

α degree	p_{fs} atm	p_m/p_{fs} Orifice # 1	2	3	4	5	(2+4+5)/3
0	.0088	1.209	1.217	1.163	1.202	1.093	1.171

CONFIGURATION BP_2 MODIFIED

M = 4.5, RE = 0.48 x 10^6/in, p_o = 5.2 atm, q = 0.254 atm

α degree	p_{fs} atm	p_m/p_{fs} Orifice # 1	2	3	4	5	(2+4+5)/3
0	.0176	1.073	1.085	1.089	1.085	1.046	1.072

CONFIGURATION BP_2 MODIFIED

M = 4.5, RE = 0.24 x 10^6/in, p_o = 2.61 atm, q = 0.127 atm

α degree	p_{fs} atm	p_m/p_{fs} Orifice # 1	2	3	4	5	(2+4+5)/3
0	.0086	1.246	1.238	1.198	1.198	1.143	1.193

TABLE IV (Contd)

Pressure on Side-On Blast Gage When Placed in Supersonic Wind Tunnel

CONFIGURATION BP_2 MODIFIED W/SAND (1)

M_{fs} = 4.5, RE = 0.48 x 10^6/in, p_o = 5.2 atm, q = 0.254 atm

α degree	p_{fs} atm	p_m/p_{fs} Orifice #					
		1	2	3	4	5	(2+4+5)/3
0	.0180	1.098	1.121	-	-	-	-

CONFIGURATION BP_2 MODIFIED W/SAND (1)

M_{fs} = 4.5, RE = 0.24 x 10^6/in, p_o = 2.61 atm, q = 0.127 atm

α degree	p_{fs} atm	p_m/p_{fs} Orifice #					
		1	2	3	4	5	(2+4+5)/3
0	.0090	1.220	1.212	-	-	-	-

CONFIGURATION BP_2 MODIFIED W/SAND (2)**

M_{fs} = 4.5, RE = 0.48 x 10^6/in, p_o = 5.2 atm, q = 0.254 atm

α degree	p_{fs} atm	p_m/p_{fs} Orifice #					
		1	2	3	4	5	(2+4+5)/3
0	.0180	1.163	-	-	-	-	-

CONFIGURATION BP_2 MODIFIED W/SAND (2)**

M_{fs} = 4.5, RE = 0.24 x 10^6/in, p_o = 2.61 atm, q = 0.127 atm

α degree	p_{fs} atm	p_m/p_{fs} Orifice #					
		1	2	3	4	5	(2+4+5)/3
0	.0090	1.182	-	-	-	-	-

** *Sand is No. 20.*

TABLE V

Configuration of Blast Gage

1. Configuration B - No modification.

2. Configuration B Modified - Shaft on gage reduced (compare Figures 3-1 and 3-2).

3. Configuration B* Modified - Same as Configuration B Modified except for stainless steel tubes to orifices of gage.

4. Configuration BS_1 - Basic gage with 1/2" spike.

5. Configuration BS_2 - Basic gage with 1" spike.

6. Configuration BS_3 - Basic gage with 1 1/2" spike.

7. Configuration BS_4 - Basic gage with 2" spike.

8. Configuration BS_4^* Modified - Basic gage with 2" spike with modified shaft and stainless steel lining.

9. Configuration BP_1 Modified - Plate 5/8" long with modified shaft.

10. Configuration BP_2 - Plate 1 1/8" long.

11. Configuration BP_2 Modified - Plate 1 1/8" long with modified shaft.

12. Configuration BP_2 Modified w/sand (1) - same as BP_2 Modified but blasted with No. 80 grit on forward portion and No. 40 grit on strut.

13. Configuration BP_2 Modified w/sand (2)** - same as BP_2 Modified w/sand 1 except sand on ground 5/8" replaced with No. 20 grit.

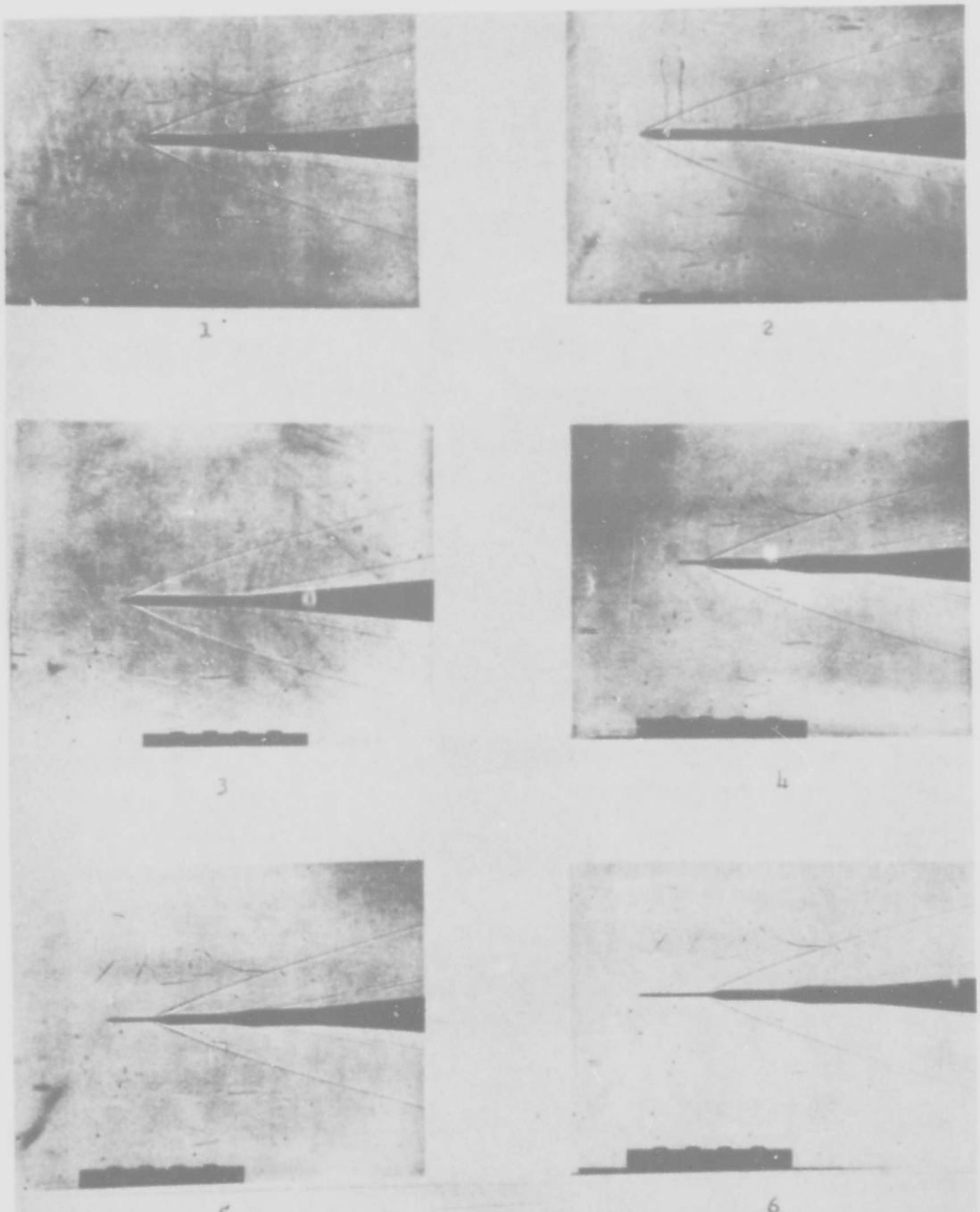

FIGURE 4 - FLOW AT MACH 4.5 OVER BRL PANCAKE GAGE WITH AND WITHOUT MODIFICATION IN SUPERSONIC WIND TUNNEL. FLOW IS FROM LEFT TO RIGHT.

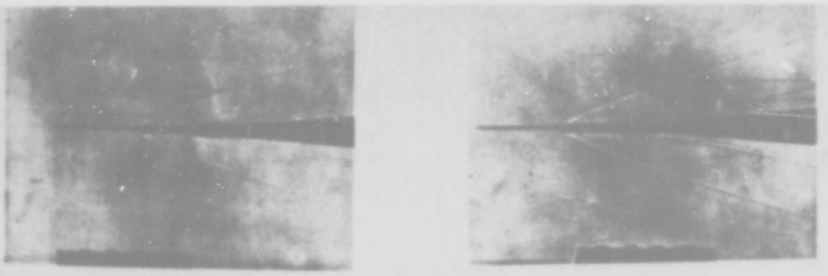

7

8

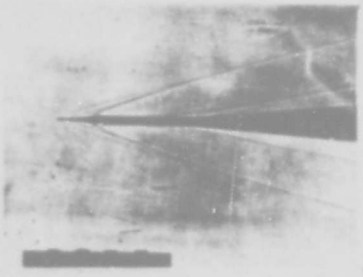

9

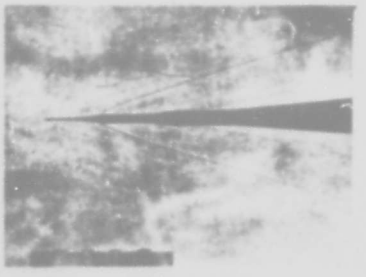

10

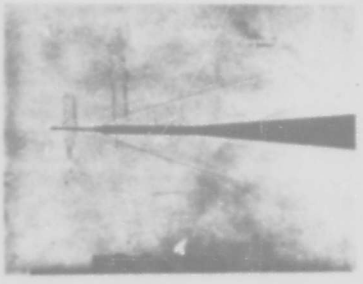

11

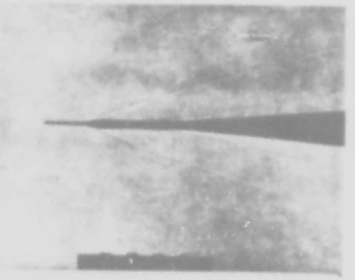

12

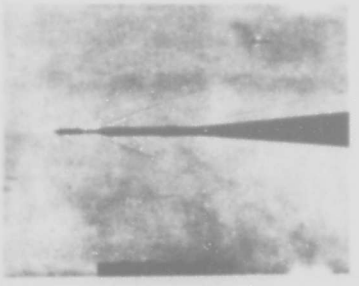

13

FIGURE 5 - FLOW AT MACH 4.5 OVER BRL PANCAKE GAGE WITH AND WITHOUT MODIFICATION IN SUPERSONIC WIND TUNNEL. FLOW IS FROM LEFT TO RIGHT.

Computations of pressure over a 15° wedge plane[4] and experimental pressures over a double wedge plane[5] are given in Table VI. The double wedge plane is at an angle of attack of 1°.

Pressure ratios for the flat plane surface of an airfoil with a plano-convex cross section (cambered airfoil) are reported from Reference 6 and tabulated in Table VII. Table VIII gives the scaled distances for these pressures at two distances along each airfoil. The thickness ratio is the actual ratio instead of the ratio of maximum thickness to distance along the chord. Table IX gives the pressure ratio of flow over a symmetrical circular arc.[7] The pressures were computed from the smooth curves of local flow velocities. Table X is the pressure gradient at maximum thickness of the circular arc.

ANALYSIS OF DATA

The pressure ratios for measurements of pressure on the unmodified pancake gage have been plotted against a scaled distance $\frac{1}{M_{fs}^3} \frac{s_n + s_o}{\tau}$ in Figure 6. This graph shows that the ratios are a function of both the Reynolds number and the Mach number for mass flows greater than Mach 1. The cross, triangle and square denote the pressure ratio on the air blast gage at orifices 1, (2,4,5) and 3 respectively. These are positions from the front to the rear of the gage. Measurements at the middle point (triangle) are average values for all measurements made at the middle of the chord of the gage. The aerodynamic error introduced by the measuring devices in Figure 6 is $\frac{p_m}{p_{fs}} - 1$. The deviations of the curves and points from $\frac{p_m}{p_{fs}} = 1$ show the aerodynamic effect for both subsonic and supersonic flow. The curves for the supersonic measurements should not be extrapolated to the right for the pressure ratios should decrease without limit as $\frac{u_{fs}}{a_{fs}}$ approaches 1. This also occurs as $\frac{u_{fs}}{a_{fs}}$ approaches 1 from the left.

TABLE VI

Computed Pressure Distributions for 15° Wedge Plane
and Experimental Pressure Distribution
for Double Wedge Plane

Wedge Plane*

M	ϵ		s_a	s_b	p_m/p_{fs}
2.5	15.05	1.4	1.87	11.6	1.012
4.5	15.00	1.4	1.89	11.0	1.027
7.5	15.18	1.4	1.87	10.5	1.120

Double Wedge Plane**

$\frac{s_n+s_o}{2s_o}$	$\frac{s_n+s_o}{\tau}$	p_m/p_{fs}	
		M	
		1.22	1.47
.1	-	1.50	1.39
.2	6.7	1.17	1.10
.3	10	1.20	1.10
.4	13	1.25	1.10
.5	17	1.21	1.09
.6	20	1.18	1.09
.7	-	1.05	- .98
.8	-	1.06	1.04
.9	-	1.07	1.13

* *Pressure ratio constant at* $s_a \leq \frac{s_n + s_o}{\tau} \leq s_b$.

** *Ratio of thickness to length is 0.03.*

ϵ = *wedge half angle.*

TABLE VII

Observed Values of $(p_m - p_{fs})/p_{fs}$ on Flat Surface of 6 Airfoils

Profile No.	Station	s_n+s_o	$(p_m - p_{fs})/p_{fs}$ M .5	.65	.80	.95	1.08
1	8	.050	-.1320	-.2059	-.3266	-.5650	-.5142
	9	.100	-.1027	-.1659	-.2683	-.4795	-.4399
	10	.200	-.0368	-.0722	-.1577	-.3348	-.3208
	11	.400	.0030	.0044	-.0081	.0278	-.3395
	12	.600	.0074	.0192	.0278	.0474	-.0245
	13	.850	.0143	.0308	.0524	.0164	.1020
2	8	.050	-.1188	-.1843	-.2930	-.6508	-.6170
	9	.100	-.1085	-.1713	-.2715	-.4947	-.4595
	10	.200	-.0578	-.1171	-.1882	-.3904	-.3697
	11	.400	.0030	.0006	-.0215	.0094	-.3526
	12	.600	.0089	.0204	.0237	.0486	-.0832
	13	.850	.0191	.0376	.0573	.0120	.0645
3	8	.050	-.1102	-.1627	-.2612	-.600	-.5607
	9	.100	-.1139	-.1718	-.2661	-.5560	-.5101
	10	.200	-.0662	-.1251	-.1949	-.3974	-.3828
	11	.400	-.0002	-.0095	-.0533	-.0107	-.3789
	12	.600	.0103	.0240	.0161	.0632	-.0988
	13	.850	.0205	.0405	.0546	.0057	.0530
4	8	.050	-.1022	-.1535	-.2764	-.6804	-.6652
	9	.100	-.1073	-.1594	-.2522	-.5983	-.5550
	10	.200	-.0842	-.1361	-.2074 -.0690	-.4347	-.4358
	11	.400	-.0149	-.0479	-.1057	-.0417	-.4179
	12	.600	.0126	.0198	.0009	.0423	-.0865
	13	.850	.0243	.0441	.0488	-.0133	.0408
5	8	.050	-.0928	-.1532	-.2558 -.3010	-.6849	-.6701
	9	.100	-.1059	-.1580	-.2585 -.2800	-.6274	-.5926
	10	.200	-.0859	-.1367	-.2222	-.4113	-.4767
	11	.400	-.0313	-.0636	-.1295	-.0771	-.4375
	12	.600	.0098	.0065	-.0152 .0081	.0038	.1274
	13	.850	.0264	.0447	.0206	-.0354	.0359
6	8	.050	-.0824	-.1307	-.2518	-.6937	-.706
	9	.100	-.0913	-.1467	-.2894	-.6520	-.6391
	10	.200	-.0796	-.1340	-.2348	-.3551	-.5069
	11	.400	-.0406	-.0710	-.1375 -.1026	-.0960	-.4620
	12	.600	.004	.0021	-.0412	-.0392	-.1143
	13	.850	.0285	.4407	-.0161	-.0644	-.0275

TABLE VIII

Scaled Distance on Flat Surface of Six Airfoils at Distances from Nose of 0.4 and 0.6 of Length

Profile* No.	Station	$s_n + s_o$	$\frac{1}{M^3}\frac{s_n + s_o}{\tau}$				
			.5	.65	.80	.95	1.08
1 (10%)	11	.400	33.0	15.	8.0	4.8	3.27
	12	.600	55.2	25.1	13.4	8.07	5.48
2 (12%)	11	.400	27.4	12.5	6.69	4.01	2.72
	12	.600	46.0	20.9	11.2	6.73	4.56
3 (14%)	11	.400	23.5	10.7	5.73	3.44	2.33
	12	.600	39.4	17.9	9.61	5.77	3.91
4 (16%)	11	.400	20.6	9.39	5.03	3.02	2.05
	12	.600	34.5	15.7	8.40	5.04	3.42
5 (18%)	11	.400	18.3	8.34	4.46	2.68	1.82
	12	.600	30.7	14.0	7.49	4.57	3.05
6 (20%)	11	.400	16.5	7.50	4.02	2.41	1.64
	12	.600	27.6	12.6	6.73	4.04	2.74

* Percent of ratio $\frac{\tau_{max}}{2s_o}$

TABLE IX

Pressure Distribution for Laminar Flow Over Circular Arc Airfoil of Reference 13

Size	M	$\frac{s_n+s_o}{2s_o}$	$\frac{s_n+s_o}{\tau}$	$\frac{1}{M_\infty^3}$	$\frac{s_n+s_o}{\tau}$	M_m	p_m/p_{fs}
3" x 6"	.889	.30				0.98	.90
"	"	.40				1.00	.88
"	"	.50	8.33	11.9		1.01	.88
"	"	.60				0.99	.88
"	"	.70				0.97	.91
3" x 6"	.914	.30				1.01	.92
"	"	.40				1.03	.89
"	"	.50	8.33	10.9		1.07	.84
"	"	.60				1.04	.86
"	"	.70				1.01	.92
3" x 6"	.936	.30				1.04	.89
"	"	.40				1.08	.86
"	"	.50	8.33	10.2		1.12	.82
"	"	.60				1.14	.79
"	"	.70				1.03	.92
3" x 6"	.954	.30				1.05	.90
"	"	.40				1.10	.84
"	"	.50	8.33	9.6		1.14	.80
"	"	.60				1.17	.78
"	"	.70				1.17	.78
3" x 12"	.828	.32				1.07	.83
"	"	.40				1.04	.78
"	"	.50	4.17	7.34		1.06	.78
"	"	.57				1.04	.78
"	"	.73				0.95	.88
3" x 12"	.860	.32				1.04	.81
"	"	.40				1.09	.76
"	"	.50	4.17	6.56		1.15	.72
"	"	.57				1.19	.68
"	"	.73				0.98	.88
3" x 12"	.889	.32				1.07	.81
"	"	.40				1.13	.74
"	"	.50	4.17	5.94		1.20	.69
"	"	.57				1.25	.65
"	"	.73				1.25	.65
3" x 12"	.914	.32				1.09	.82
"	"	.40				1.15	.77
"	"	.50	4.17	5.46		1.23	.69
"	"	.57				1.27	.65
"	"	.73				1.38	.56
3" x 12"	.936	.32				1.05	.89
"	"	.40				1.11	.82
"	"	.50	4.17	5.08		1.19	.75
"	"	.57				1.23	.71
"	"	.73				1.36	.59

TABLE X

Pressure Gradient at Maximum Thickness on Biconvex Circular Arc Airfoils with Turbulent Boundary Layer*

M_m	$\frac{P_{m1} - P_{m2}}{P_{m1}}$	
	6%	12%
0.97	-	.0140
0.98	-	.0145
0.99	.0065	.0150
1.00	.0065	.0155
1.01	.0070	.0160
1.02	.0075	.0175
1.03	.0080	.0190
1.04	.0090	.0205
1.05	.0120	.0225
1.06	.0215	.0245
1.064	.0230	-
1.07	.0215	.0270
1.08	.0120	.0300
1.09	-.001	.0345
1.095	-	.0350
1.10	-.0115	.0345
1.11	-	.0240
1.12	-	.0090
1.13	-	-.0060
1.14	-	-.0200

*Reference 13

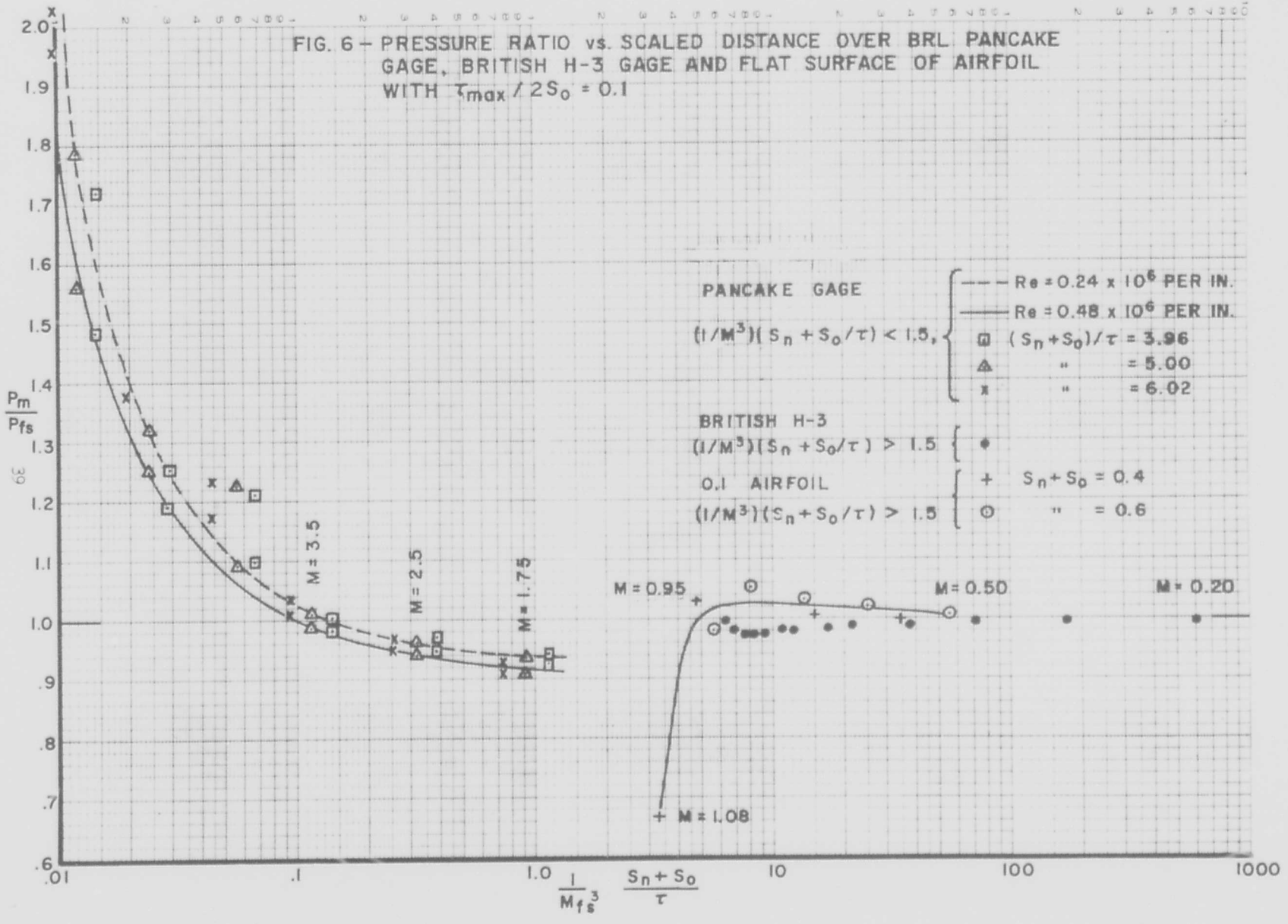
FIG. 6 – PRESSURE RATIO vs. SCALED DISTANCE OVER BRL PANCAKE GAGE, BRITISH H-3 GAGE AND FLAT SURFACE OF AIRFOIL WITH $\tau_{max}/2S_0 = 0.1$
PANCAKE GAGE
$(1/M^3)(S_n + S_0/\tau) < 1.5$
Re = 0.24 x 10^6 PER IN.
Re = 0.48 x 10^6 PER IN.
$(S_n+S_0)/\tau$ = 3.96
" = 5.00
" = 6.02
BRITISH H-3
$(1/M^3)(S_n + S_0/\tau) > 1.5$
0.1 AIRFOIL
$(1/M^3)(S_n+S_0/\tau) > 1.5$
S_n+S_0 = 0.4
" = 0.6
M = 3.5
M = 2.5
M = 1.75
M = 0.95
M = 0.50
M = 0.20
M = 1.08
$\frac{P_m}{P_{fs}}$
$\frac{1}{M_{fs}^3}$
$\frac{S_n+S_0}{\tau}$
2.0
1.9
1.8
1.7
1.6
1.5
1.4
1.3
1.2
1.1
1.0
.9
.8
.7
.6
.01
.1
1.0
10
100
1000

At the lowest supersonic Mach numbers, the error is nearly 10. percent and shows a pressure lower than free stream pressure. As the Mach number increases the suction decreases until finally the pressure is greater than free stream pressure. The error increases to more than 100 percent at the highest velocities. Figure 6 also shows that the error decreases as the position of measurement is moved further back from the leading edge of the plate.

Since it was shown in Reference 1 that in order to have the smallest error the transducer should be in a flat surface, flow conditions over a flat surface are also considered.[4,5,6] The pressure at two positions of the plate of Reference 6 is plotted in Figure 6. The positions of measurement are at 0.4 the length of the plate and in front of the position of maximum thickness and 0.6 the chord length and behind the position of maximum thickness. A smooth curve is drawn through these points and it is assumed that in the range considered this curve gives the maximum error in the pressure measurement.

The photographs in References 7 and 9 show the flow field around airfoils of various shapes. Figure 7 has been taken from Reference 9 and shows the flow field on the flat surface of an airfoil similar to that in Reference 6 and shows that there is a transition from unsteady to steady flow over most of the plate at transonic speeds. Reference 7 shows that on the circular surface of a symmetrical element the flow changes from symmetrical flow over most of the surface to asymmetrical flow with attached shocks as transonic speed approaches Mach 1. Figure 6 shows that as the flow speed approaches the speed of sound the error increases without limit. It should be noted that as shown in Reference 7 the flow speed may reach the local speed of sound without attached shocks being present.

Figures 8 and 9 show the pressure variations over the flat surfaces of six cambered airfoils at different Mach numbers for $\frac{s_n + s_o}{\tau}$ of 0.4 and 0.6 respectively. Smooth curves were drawn through points of different thickness at each flow velocity in Figures 8 and 9 to show the

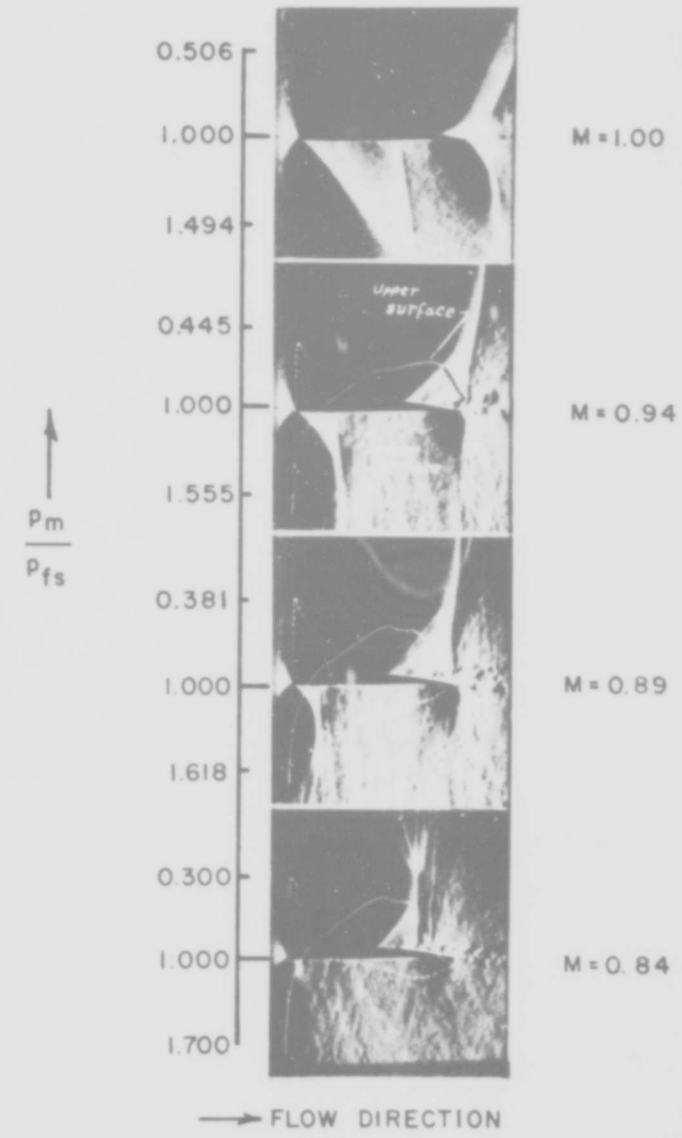

FIGURE 7. SCHLIEREN PHOTOGRAPHS OF FLOW OVER AN AIRFOIL AT ZERO ANGLE OF ATTACK SUPERIMPOSED ON CURVES OF P_m / P_{fs} VERSUS DISTANCE. THE DASHED CURVE (----) IS THE LOWER SURFACE PRESSURE AND THE SOLID CURVE (——) IS THE UPPER SURFACE PRESSURE THE LOWER SURFACE IS PLANE AND THE UPPER SURFACE IS CONVEX (NACA420)

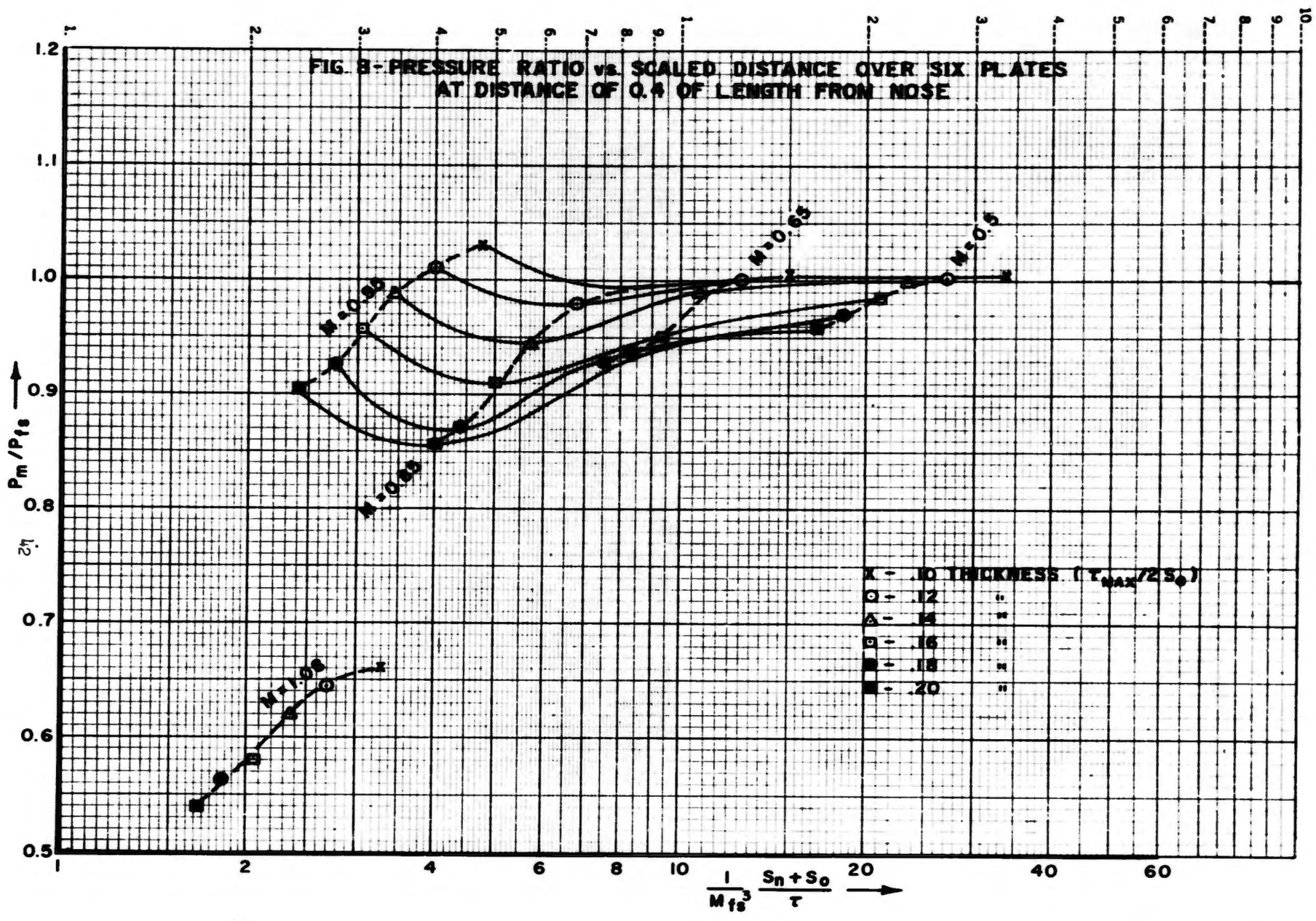
FIG. 8 - PRESSURE RATIO vs. SCALED DISTANCE OVER SIX PLATES AT DISTANCE OF 0.4 OF LENGTH FROM NOSE
P_m / P_{fs}
$\frac{1}{M_{fs}^3} \frac{S_n + S_o}{\tau}$
M = 0.65
M = 0.85
M = 1.05
M = 1.65
X - .10 THICKNESS ($\tau_{MAX}/2S_o$)
O - .12 "
Δ - .14 "
□ - .16 "
● - .18 "
■ - .20 "

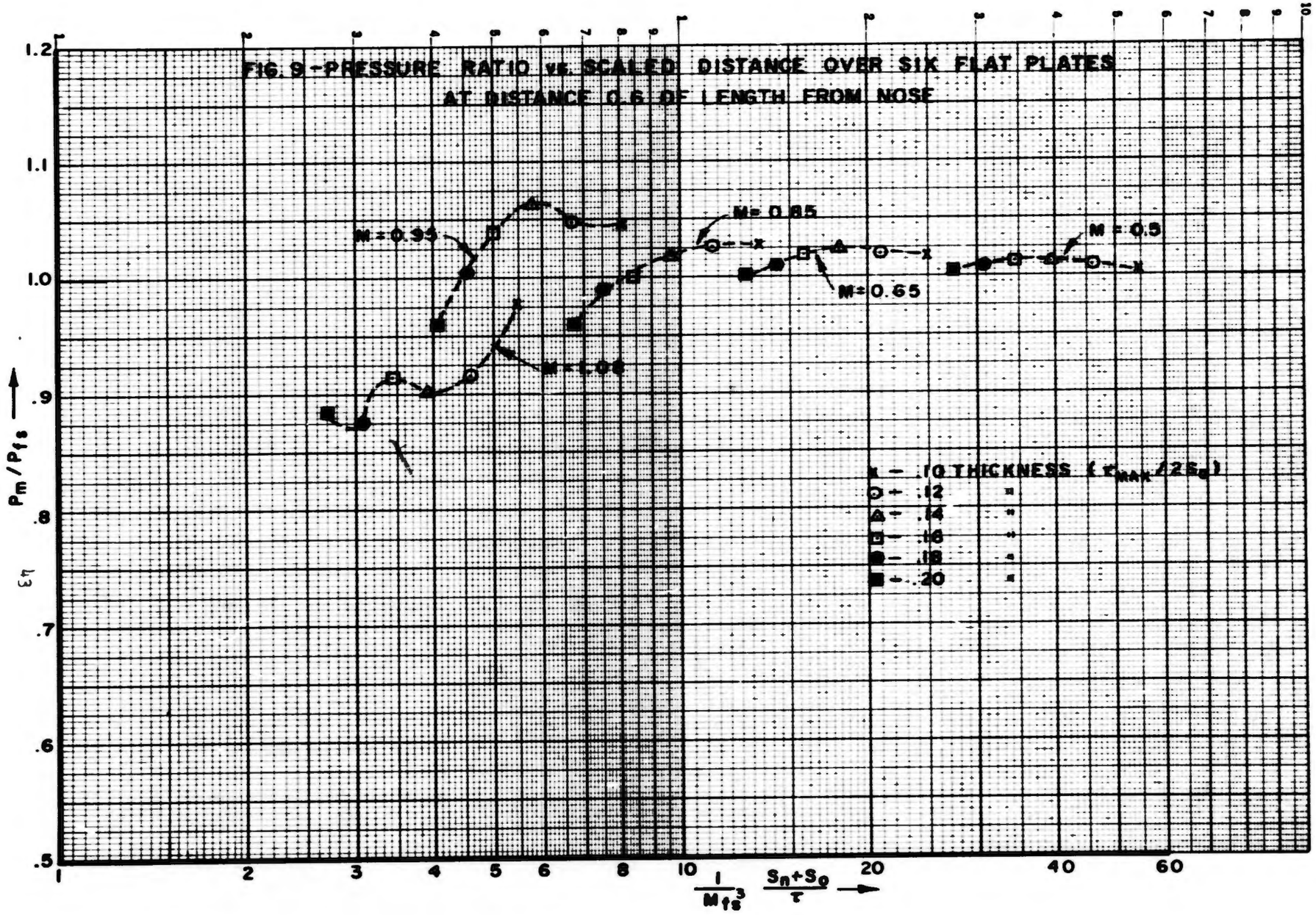
FIG. 9 - PRESSURE RATIO vs. SCALED DISTANCE OVER SIX FLAT PLATES AT DISTANCE 0.6 OF LENGTH FROM NOSE
M = 0.95
M = 0.85
M = 0.9
M = 0.65
M = 1.06
x — .10 THICKNESS (t_MAX / 2S_0)
o — .12 "
Δ — .14 "
□ — .16 "
■ — .18 "
■ — .20 "
Pm / Pfs
1/Mfs³ (Sn+So)/τ
1.2
1.1
1.0
.9
.8
.7
.6
.5
1
2
3
4
5
6
8
10
20
40
60

effect of thickness at a given flow velocity. Smooth curves were also drawn through points of different flow velocity (Mach 0.5 to 0.95) at each thickness in Figure 8 to show the effect of flow velocity at a given thickness. Due to the difficulties in reading the graph the second set of curves was not drawn in Figure 9. The large error at the very high Mach numbers would indicate that standing shocks are formed and flow over most of the surface is steady as shown in Figure 7. Tables VIII and IX show this for the point of maximum thickness of a symmetrical profile. Also shown on Figure 6 is the pressure over the H-3 British gage. These pressures are tabulated in Table XI and show error is negligible for low subsonic flow Mach numbers.

Figure 6 shows that in order to have negligible error the measurements should not be made for pressures corresponding to flow velocities near Mach 1. Figures 8 and 9 show that thickness ratio must be of the order of 0.1 or less, the ratio that was recommended in Reference 3. Since Figure 9 indicates pressure ratios for measurements behind the point of maximum thickness, these measurements should be considered when an analogue for the pancake gage is needed.

The measurements made on the gage after modification were at Mach 4.5. Table I shows that for air blast measurements this flow velocity does not exist. Figures 10 and 11 do, however, show the effects of the various modifications on the pancake gage. The notation, Configuration B means basic gage, Configuration BS is gage modified with spike and Configuration BP means gage modified with a plate. The plate attached to the gage shows the greatest decrease in pressure error over the gage. All measurements p_m/p_{fs} are larger than 1. These curves, however, magnify the effect of having the measuring device away from the leading edge.

A shock is reflected at the point where the gage is supported at the back as shown in e in Figure 1. The shaft should be as thin as the gage housing in order to eliminate this reflected wave.

TABLE XI

Pressure Ratios on Surface of British H-3 Gage

M	$\frac{1}{M^3}$	$\frac{s_n + s_o}{\tau}$	p_m/p_{fs}
.200		580	.998
.300		172	.996
.400		70	.992
.500		37	.990
.550		-	-
.600		21	.984
.650		17	.979
.701		13	.980
.726		12	.976
.752		11	.975
.777		-	-
.803		9.0	.972
.827		8.2	.972
.854		7.4	.973
.869		-	
.879		6.9	.980
.905		6.3	.995

$s_n + s_o = 1.3$ inches

$\tau = .28$ inches

FIG. 10 - PRESSURE MEASUREMENTS ON VARIOUS CONFIGURATIONS OF THE PANCAKE GAGE AT MACH 4.5 AND $R_\theta = .48 \times 10^6$ PER INCH. (SEE TABLE 3 FOR CONFIGURATION DESCRIPTION)

1. BASIC GAGE (NO MODIFICATION).
2. SHAFT ON GAGE 1 ABOVE IS REDUCED.
3. SAME AS GAGE 2 ABOVE EXCEPT FOR STAINLESS TUBES TO ORIFICES.
4. GAGE 1 MODIFIED WITH 1/2" SPIKE.
5. GAGE 1 MODIFIED WITH 1" SPIKE.
6. GAGE 1 MODIFIED WITH 1 1/2" SPIKE.
7. GAGE 1 MODIFIED WITH 2" SPIKE.
8. GAGE 2 MODIFIED WITH 2" SPIKE.
9. GAGE 2 MODIFIED WITH 5/8" PLATE.
10. GAGE 1 MODIFIED WITH 1 1/8" PLATE.
11. GAGE 2 MODIFIED WITH 1 1/8" PLATE.

$\frac{S_n + S_a}{\tau} = 3.96$

$\frac{S_n + S_a}{\tau} = 5.00$

$\frac{S_n + S_a}{\tau} = 6.05$

$\frac{P_m}{P_{fs}}$

$\frac{1}{M_{fs}^3}$ $\frac{S_n - S_a}{\tau}$

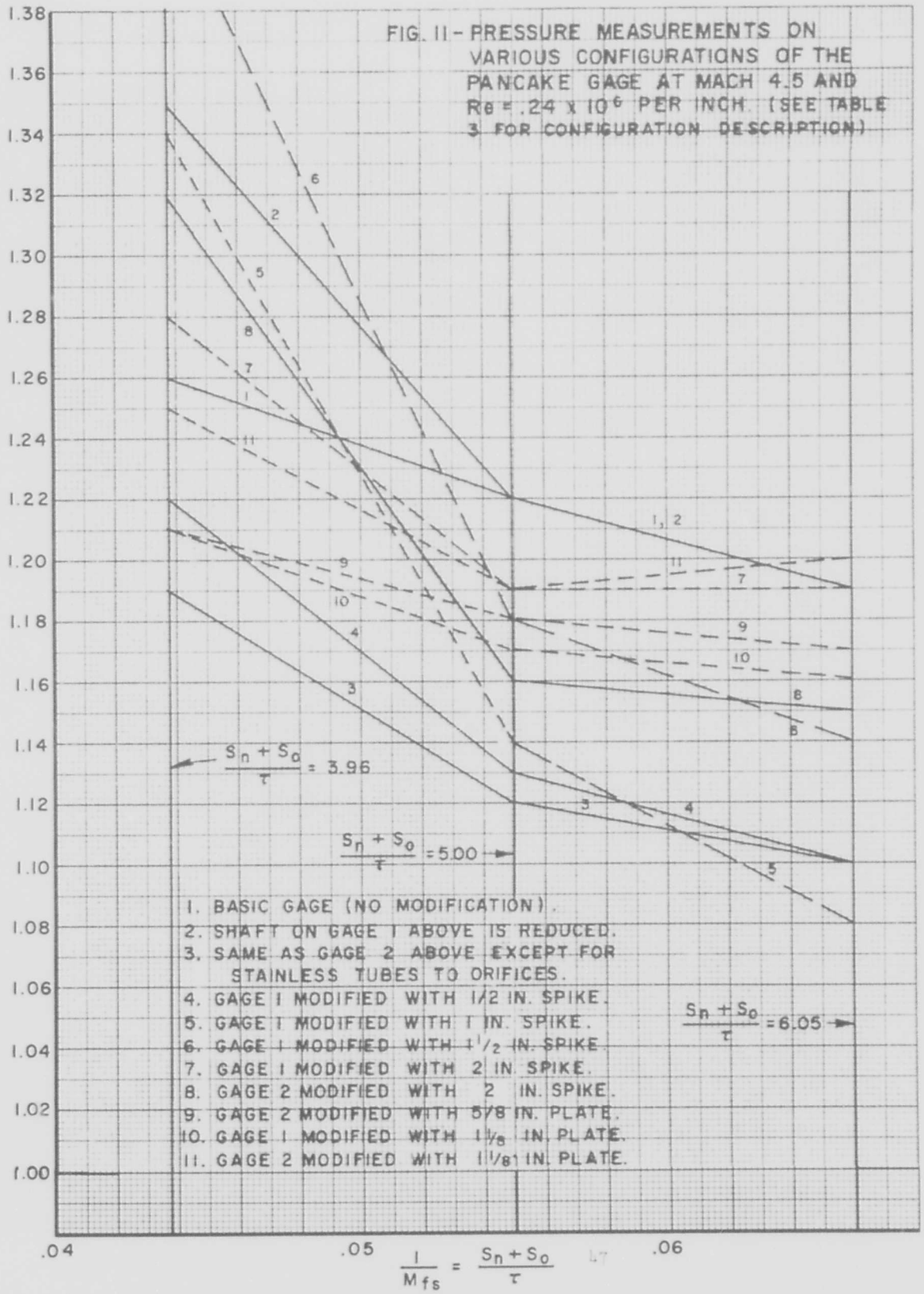
FIG. 11 - PRESSURE MEASUREMENTS ON VARIOUS CONFIGURATIONS OF THE PANCAKE GAGE AT MACH 4.5 AND Re = .24 x 10^6 PER INCH. (SEE TABLE 3 FOR CONFIGURATION DESCRIPTION)
1.38
1.36
1.34
1.32
1.30
1.28
1.26
1.24
1.22
1.20
1.18
1.16
1.14
1.12
1.10
1.08
1.06
1.04
1.02
1.00
.04
.05
.06
1/Mfs = (Sn + So)/τ
(Sn + So)/τ = 3.96
(Sn + So)/τ = 5.00
(Sn + So)/τ = 6.05
1. BASIC GAGE (NO MODIFICATION).
2. SHAFT ON GAGE 1 ABOVE IS REDUCED.
3. SAME AS GAGE 2 ABOVE EXCEPT FOR STAINLESS TUBES TO ORIFICES.
4. GAGE 1 MODIFIED WITH 1/2 IN. SPIKE.
5. GAGE 1 MODIFIED WITH 1 IN. SPIKE.
6. GAGE 1 MODIFIED WITH 1 1/2 IN. SPIKE.
7. GAGE 1 MODIFIED WITH 2 IN. SPIKE.
8. GAGE 2 MODIFIED WITH 2 IN. SPIKE.
9. GAGE 2 MODIFIED WITH 5/8 IN. PLATE.
10. GAGE 1 MODIFIED WITH 1 1/8 IN. PLATE.
11. GAGE 2 MODIFIED WITH 1 1/8 IN. PLATE.

RESPONSE OF FINITE GAGE

The problem considered is that of the response of a gage element of finite size to pressure pulses of triangular and Friedlander form. The plane element is orientated with the axis parallel to the direction of propagation of the shock. The shock front position on circular or rectangular crystal at time t is shown in Figure 12. The end function differs according to how the pulse is terminated (Figure 13).

The pressure pulses are:

$$\begin{aligned} P &= 0 \qquad\qquad , t < 0 \\ P &= \left(1 - \frac{t}{\theta_1}\right), \; t \geq 0, \end{aligned} \tag{1}$$

and

$$\begin{aligned} P &= 0 \qquad\qquad\qquad , t < 0 \\ P &= \left(1 - \frac{t}{\theta_1}\right) e^{-\frac{t}{\theta_2}} , \; t \geq 0 \end{aligned} \tag{2}$$

where (1) is the triangular form and (2) is the Friedlander form with two constants. The pressure P is the ratio of excess pressure to peak excess pressure at shock front. Another form, the modified Friedrich equation[10] has not been considered. If the pulses are terminated, $P = 0$ for $t > \theta_1$.

It is assumed that the pulse does not change its form while traveling over the piezoelectric element, Figure 14. Also, the wave velocity is constant and wave length is equal to or longer than the element. The distance $R - R_o$ is denoted by s to facilitate integration and is measured from the center of gage.

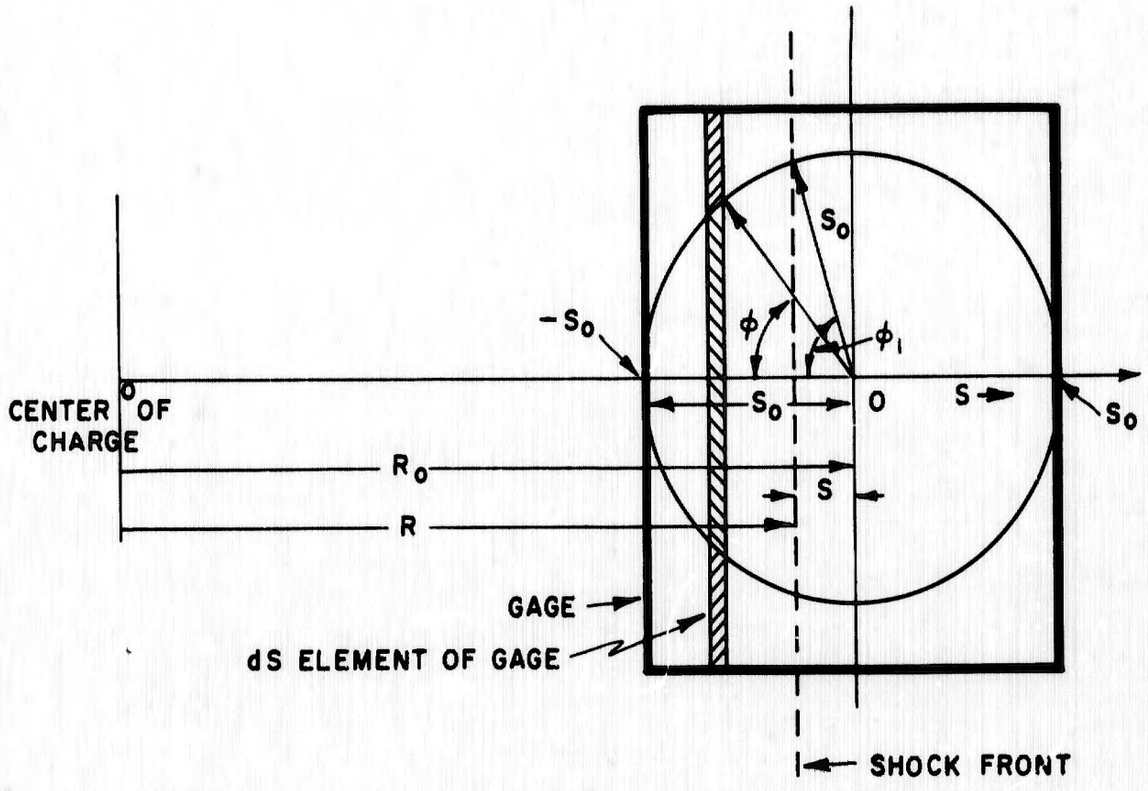

FIGURE 12 - SHOCK FRONT PROPAGATING ACROSS A RECTANGULAR OR CIRCULAR CRYSTAL

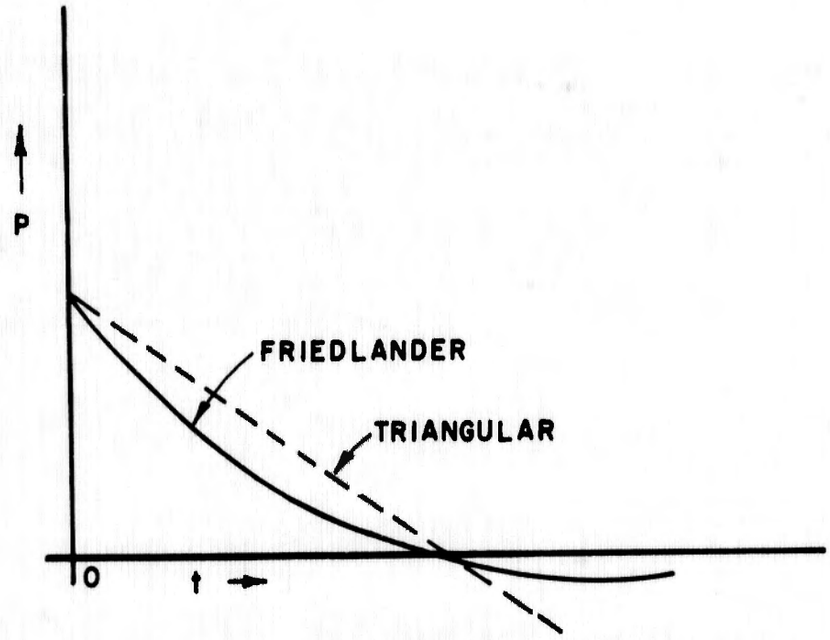

(a) NON-TERMINATED WAVES

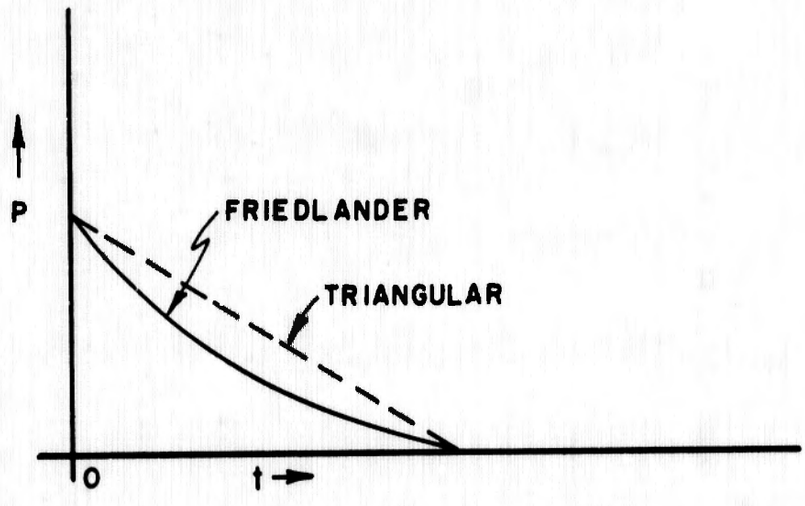

(b) TERMINATED WAVES

FIGURE 13-ASSUMED FORMS OF PRESSURE PULSES

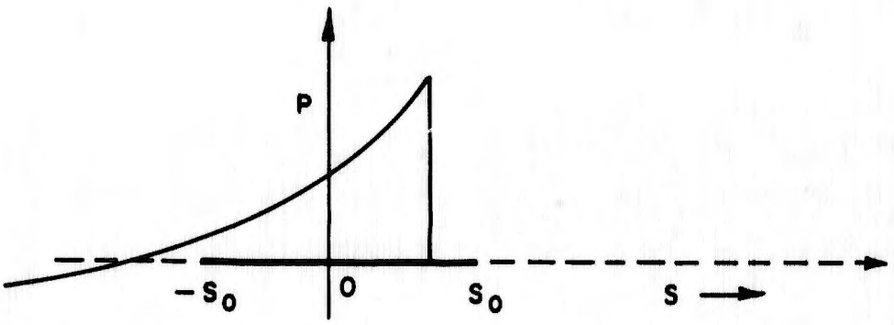

$$-\frac{S_0}{U} \le t \le \frac{S_0}{U}$$

(a) SHOCK FRONT ON GAGE SURFACE AND TAIL OF SHOCK OFF SURFACE

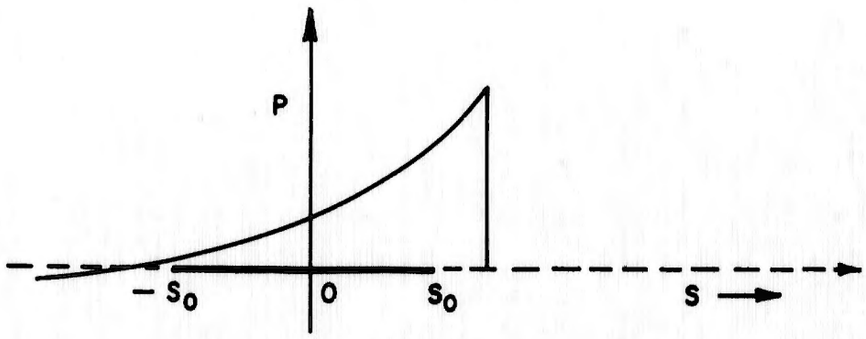

$$\frac{S_0}{U} \le t \le \theta_1 - \frac{S_0}{U}$$

(b) SHOCK FRONT AND TAIL OF SHOCK OFF GAGE SURFACE

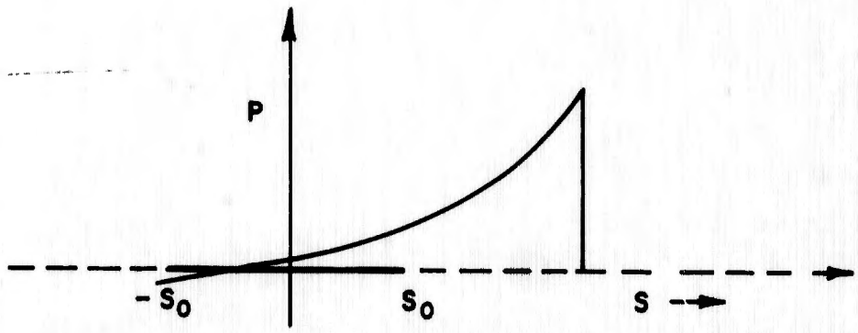

$$\theta_1 - \frac{S_0}{U} \le t \le \theta_1 + \frac{S_0}{U}$$

(c) SHOCK FRONT OFF GAGE SURFACE BUT TAIL OF SHOCK ON GAGE SURFACE

FIGURE 14 – PRESSURE PULSE WITH DURATION θ, PROPAGATING ACROSS GAGE OF LENGTH $2S_0$

The response is defined as the electric output, for a piezoelectric gage ratio of electric charge, to applied force. It is assumed that the charge is proportional to applied force on the element. If at s = 0, t = 0, the pressure on a rectangular element is

$$p_1(t) = \frac{K}{2s_o L} \int_{-\frac{s_o}{U}}^{t} P(t - t_o)\, dA(t_o)$$

$$\frac{s_o}{U} \leq t \leq \frac{s_o}{U},$$

$$p_2(t) = \frac{K}{2s_o L} \int_{\frac{s_o}{U}}^{\frac{s_o}{U}} P(t - t_o)\, dA(t_o) \qquad (3)$$

$$\frac{s_o}{U} \leq t \leq \theta - \frac{s_o}{U},$$

$$p_3(t) = \frac{K}{2s_o L} \int_{t - \theta}^{\frac{s_o}{U}} P(t - t_o)\, dA(t_o)$$

$$\theta - \frac{s_o}{U} \leq t \leq \theta + \frac{s_o}{U},$$

when the pulse is terminated.

If the wave is not terminated, the domain of the second expression becomes $\frac{s_o}{U} \leq t \leq T_1$ and the third expression does not appear. The static response is

$$p_s = KA_g P_c. \qquad (4)$$

P_c is known pressure applied to gage of area A_g.

The impulse which is

$$I(t_o) = \int_{-\frac{s_o}{U}}^{t_o} P(t - t_o)\, dt \tag{5}$$

is determined by integrating the pressure over time. Figure 12 shows that the domain of integration must be separated into three parts when the wave is terminated, hence impulse becomes

$$\int_{-\frac{s_o}{U}}^{\Theta + \frac{s_o}{U}} \sum_{i=1}^{3} p_i\, dt = \frac{K}{2s_o L} \int_{-\frac{s_o}{U}}^{\Theta + \frac{s_o}{U}} \int_{-\frac{s_o}{U}}^{\frac{s_o}{U}} P(t - t_o)\, dA(t_o)\, dt. \tag{6}$$

When the wave is not terminated, the integral is separated into two parts.

If, however, before $t = -\frac{s_o}{U}$ and after $t = \Theta + \frac{s_o}{U}$, $P = 0$, the order of integration may be interchanged so that

$$\int_{-\frac{s}{U}}^{\Theta + \frac{s_o}{U}} \sum_{i=1}^{3} p_i\, dt = KI. \tag{7}$$

If for $t > \Theta + \frac{s_o}{U}$, $P < 0$ the above integral is less than KI.

W. Fader[11] computed the force and impulse on a rectangular plate for a terminated triangular wave. The force was

$$p_1(t) = \frac{KU}{2s_o}\left\{\frac{s_o}{U} - \frac{s_o^2}{2\Theta U^2} - \frac{t^2}{2\Theta} + t - \frac{s_o t}{\Theta U}\right\}$$

$$-\frac{s_o}{U} \leq t \leq \frac{s_o}{U},$$

$$p_2(t) = K\left(1 - \frac{t}{\Theta}\right) \qquad (8)$$

$$\frac{s_o}{U} \leq t \leq \Theta - \frac{s_o}{U}$$

$$p_3(t) = \frac{KU}{2s_o}\left\{\frac{\Theta}{2} + \frac{s_o}{U} + \frac{s_o^2}{2\Theta U^2} + \frac{t^2}{2\Theta} - t - \frac{s_o t}{\Theta U}\right\}$$

$$\Theta - \frac{s_o}{U} \leq t \leq \Theta + \frac{s_o}{U}$$

Fader showed that the impulse for a rectangular plate of finite size is

$$I = K\frac{\Theta}{2} \qquad (9)$$

Hence impulse is independent of size. This result was shown in Equation (7) and indicates that the treatment of Fader is general and holds for any wave without a negative phase, but is in orrect for an actual transient shock in air.

When a circular element is considered the pressure

$$p_1(t) = K\left(\frac{\Phi_1}{\pi} - \frac{\sin \Phi_1 \cos \Phi_1}{\pi} + \frac{s_o}{\pi U\theta} \Phi_1 \cos \Phi_1 \right.$$

$$\left. - \frac{s_o}{\pi U\theta} \sin \Phi_1 + \frac{s_o}{\pi U\theta} \frac{\sin^3 \Phi_1}{3}\right),$$

$$-\frac{s_o}{U} \leq t \leq +\frac{s_o}{U}$$

$$p_2(t) = K\left(1 - \frac{t}{\theta} + \frac{s_o}{U\theta}\right), \tag{10}$$

$$\frac{s_o}{U} < t \leq \theta - \frac{s_o}{U} .$$

$$p_3(t) = K\left(\frac{s_o}{U} \cos \Phi_1 - \frac{s_o}{\pi U\theta} \Phi_1 \cos \Phi_1 \right.$$

$$\left. + \frac{1}{2} \frac{s_o}{\pi U\theta} \sin 2\Phi_1 \cos \Phi_1 + \frac{2s_o}{\pi U\theta} \frac{\sin^3 \Phi_1}{3}\right),$$

$$\theta - \frac{s_o}{U} \leq t \leq \theta + \frac{s_o}{U} .$$

The impulse is

$$I = K \int_0^{\frac{2s_o}{U}} \left(\sum_{i=1}^{3} P_i(t) \right) dt = K \frac{\theta}{2} . \tag{11}$$

Hence the impulse is also independent of the element shape for a terminated triangular wave.

When the wave form is of the Friedlander form the impulse is $K\,\theta\,e^{-1}$ for a terminated wave over a rectangular plate.

Wesley Curtis has made measurements on spherical Pentolite for positive and negative impulse and duration (Table XII). The negative duration is always longer than positive duration by a factor of two or more. Table XIII shows the time of maximum negative pressure (time of minimum pressure). This time is plotted in Figure 15 along with the duration for 1 and 5-pound explosive charges. The measurements of Curtis indicate that in computing response and impulse of explosive charges the computations should be for nonterminated waves.

A nonterminated wave of triangular form over a rectangular plate applies forces on the gage

$$p_1(t) = \frac{KU}{2s_o}\left\{t + \frac{s_o}{U} - \frac{t^2}{2\theta} - \frac{t\,\frac{s_o}{U}}{\theta} - \frac{\left(\frac{s_o}{U}\right)^2}{2\theta}\right\},$$

$$-\frac{s_o}{U} \le t \le \frac{s_o}{U},$$

(12)

$$p_2(t) = K\left(1 - \frac{t}{\theta}\right),$$

$$t \ge \frac{s_o}{U}.$$

The impulse

$$I = \frac{KU}{2s_o}\int_{-\frac{s_o}{U}}^{\frac{s_o}{U}} dt_o \int_{t_o - \frac{s_o}{U}}^{T_1} P(t - t_o)\,dt,$$

(13)

$$= \frac{K}{2}\left\{2T_1 - \frac{T_1^2}{\theta} - \frac{1}{3\theta}\left(\frac{s_o}{U}\right)^2\right\}.$$

TABLE XII

Experimental Shock Parameters for Five Pound Spherical Pentolite

$R_o/W^{1/3}$ ft/lb$^{1/3}$	I msec/in^2		Δt msec	
	Positive	Negative	Positive	Negative
4.98	18.26	26.97	1.97	15.6
5.07	16.83	22.31	1.94	16.7
5.10	17.23	25.83	1.82	19.1
5.99	15.62	19.63	2.26	16.6
7.27	13.12	15.75	2.79	17.4
8.09	11.66	12.33	2.98	16.0
8.12	11.27	16.06	3.91	16.1
8.42	11.87	12.46	3.15	15.8
9.57	10.76	9.83	3.46	13.6
11.17	8.77	8.29	3.65	16.4
11.25	8.93	9.36	3.98	17.2
11.63	8.82	9.14	3.84	15.8
14.5	6.82	5.77	4.22	12.3
20.2	5.03	3.78	4.81	11.7
29.2	3.40	-	5.33	-
40.6	2.59	-	5.80	-

TABLE XIII

Average Time to Maximum Negative Pressure

$R_o/W^{1/3}$ ft/lb$^{1/3}$	$\bar{t}$ msec/lb$^{1/3}$
5.04	3.20
6.05	3.48
7.33	4.18
8.50	4.32
9.72	4.66
11.76	5.07
14.71	5.46
20.51	6.15
29.52	6.60
41.10	6.00

FIG. 15-DURATION FOR ONE AND FIVE POUND EXPLOSIVE (Δt) AND TIME TO MAXIMUM NEGATIVE PRESSURE ($\bar{t}$)

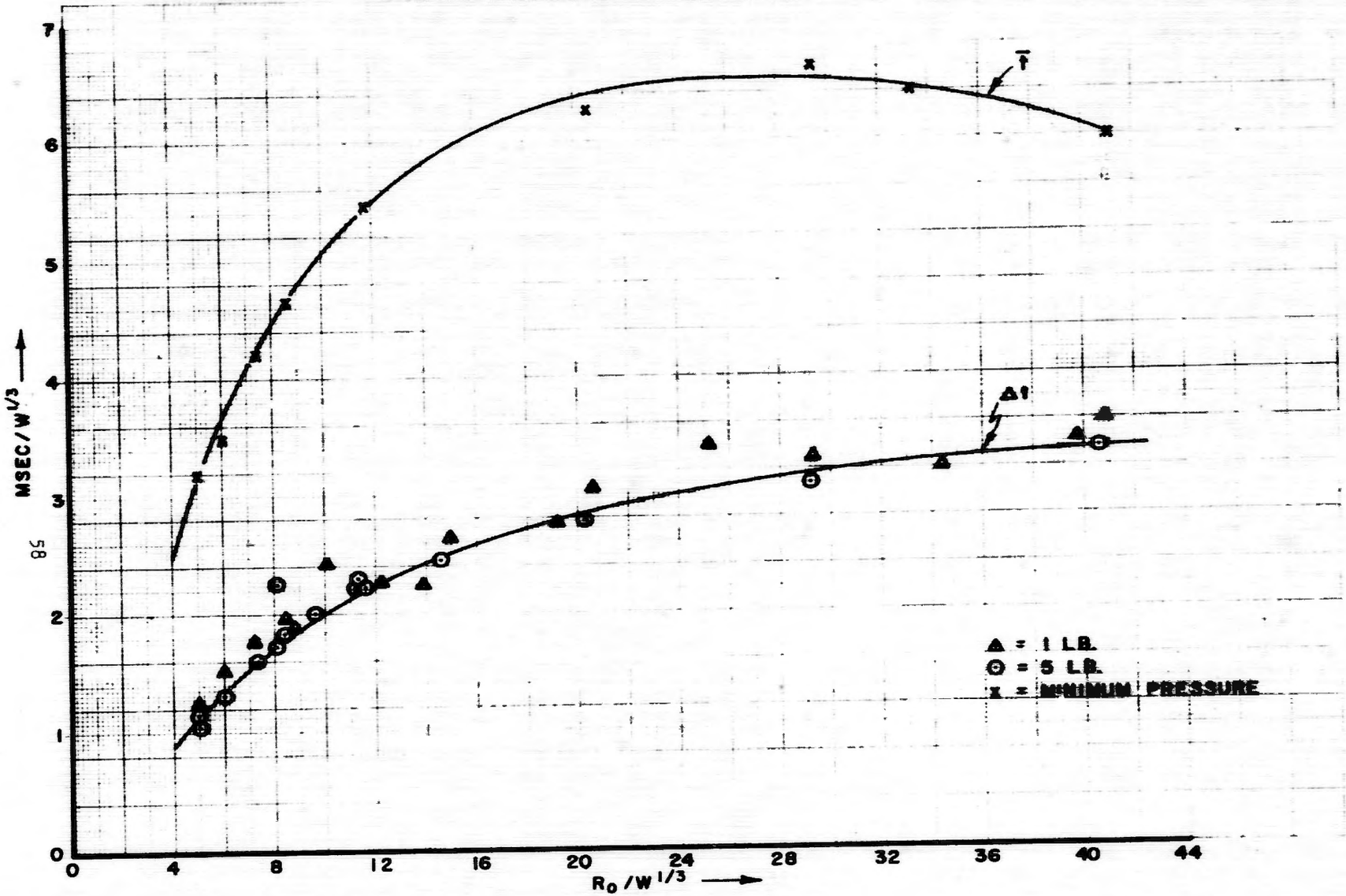

The nonterminated Friedlander form with two constants has response

$$p_1(t) = \frac{KU}{2s_o} \int_{\frac{s_o}{U}}^{t} \left(1 - \frac{t - t_o}{\theta_1}\right) e^{-\frac{t - t_o}{\theta_2}} \, dt_o$$

$$= \frac{KU}{2s_o} e^{-\frac{t}{\theta_2}} \left[\frac{\theta_2}{\theta_1} e^{-\frac{s_o}{U\theta_2}} \left(t + \frac{s_o}{U} + \theta_2 - \theta_1\right) + \theta_2 - \frac{\theta_2^2}{\theta_1}\right], -\frac{s}{U} \leq t \leq \frac{s_o}{U}, \tag{14a}$$

and

$$p_2(t) = \frac{KU}{2s_o} e^{-\frac{t}{\theta_2}} \left[\left(e^{-\frac{s_o}{U\theta_2}} - e^{\frac{s_o}{U\theta_2}}\right)\left(\frac{\theta_2}{\theta_1} t + \frac{\theta_2^2}{\theta_1} - \theta_2\right)\right.$$

$$\left. + \left(e^{-\frac{s_o}{U\theta_2}} + e^{\frac{s_o}{U\theta_2}}\right) \frac{\theta_2}{\theta_1} \frac{s_o}{U}\right], \quad t > \frac{s}{U}. \tag{14b}$$

If $\theta_2 = \theta_1 = \theta$.

$$p_1(t) = \frac{KU}{2s_o} e^{-\frac{t}{\theta}} \left[e^{-\frac{s_o}{U\theta}} \left(t + \frac{s_o}{U}\right)\right], \tag{15a}$$

and

$$p_2(t) = \frac{KU}{2s_o} e^{-\frac{t}{\theta}} \left[\left(e^{-\frac{s_o}{U\theta}} - e^{\frac{s_o}{U\theta}}\right) t\right.$$

$$\left. + \left(e^{-\frac{s_o}{U\theta}} + e^{\frac{s_o}{U\theta}}\right) \frac{s_o}{U}\right]. \tag{15b}$$

The response to the Friedlander form of pulse by plates of variable area such as circles and ellipses require numerical integration to evaluate the integral. However, when the front of the shock is on a circular element the response is

$$p_1(t) = 2 s_o^2 \int_0^{\phi_1} \{1 - \frac{t}{\theta} + \frac{s_o}{U\theta} \cos\theta - \frac{s_o}{U\theta} \cos\phi\}$$
$$\{\exp(-\frac{t}{\theta} + \frac{s_o}{U\theta} \cos\theta - \frac{s_o}{U\theta} \cos\phi)\} \sin^2\theta \, d\theta \qquad (16)$$
$$= -2U\theta s_o e^{-\frac{t}{\theta}} \{1 - \frac{t}{\theta} - \frac{s_o}{U\theta} \cos\phi\} \sin\phi$$
$$+ \frac{2s_o^2}{3U\theta} e^{-\frac{t}{\theta}} \sin^3\phi \, .$$

From the evaluated integral it can be shown that the duration of the pulse of the triangular shape must be at least 5 times the crossing time of the gage if the peak of pulse is 90 percent or more of its true maximum. For the Friedlander form the duration must be at least 10 times the crossing time of the sensing element.

DESIRED FREQUENCIES OF MEASURING ENSEMBLE

The characteristics desired of a piezoelectric gage are: linearity, freedom from frequency dependent and non-linear hysteresis, thermal stability, ruggedness, adequate high frequency response, minimum distortion and simplicity. Recently Z cut Tourmaline has been used to measure pressures up to 21 kilobars with no evidence of hysteresis or mounting effects.[14]

A distortion of the pressure pulse may be caused by an insufficient time constant or frequency response of the gage circuit, low frequency response of the oscillograph or amplifier, as well as to distortion

due to the gage size. The modern cathode ray oscillograph, itself, is quite free from resonance effects, being equally sensitive over a wide range of frequencies and will indicate with adequate fidelity the change in electric charge produced by an impulsive load on a piezoelectric crystal.

The time constant of the gage circuit must be large compared to the duration of the pulse considered, whereas the time constant of the amplifier must be small compared with the duration of the pulse considered. Therefore, in order to reproduce the signal to a high degree of accuracy, the ensemble (gage, cable, amplifier oscillograph) must be considered when computing response.

The gage must be so constructed that the period of its lowest mode of vibration must be small (fundamental frequency high) compared to the duration of the pulse considered. The fundamental frequencies of thin circular plates have been calculated using the equation [17]

$$\omega = (1.015)^2 \frac{\pi^2 \tau}{s_o^2} \left\{\frac{\mu(\lambda + \mu)}{3\rho(\lambda + 2\mu)}\right\}^{1/2}$$

where τ is thickness, s_o is radius, μ is modulus of rigidity, E is Young's modulus, ρ is density, $\lambda = \mu(E + 2\mu)\ (3\mu - E)^{-1}$ and $\omega = 2\pi f$ where f is the frequency. These frequencies are tabulated below.

Fundamental Free Vibrating Frequencies for Thin Circular Plates

Metal	Thickness inches	Frequencies (kilocycles/sec)						
		Diameter (inches)						
		0.250	0.375	0.500	0.625	0.750	0.875	1.000
Steel .36	.050	304.8	135.7	76.4	49.2	33.9	25.1	19.1
Steel .63	.050	298.6	133.0	74.8	48.2	33.2	24.5	18.7
Brass	.050	198.2	88.3	49.6	32.0	22.0	16.2	12.4

The periods of these plates are low, by a factor of ten, compared to the duration of pulses in the range of $R_o/W^{1/3} = 4$ to $R_o/W^{1/3} = 40$ as computed for 1/8 and 1/2 pound as computed from values on Figure 15.

The frequency response of the oscillograph presently being used is approximately 250 kilocycles. Since the diaphragms have frequencies of a much lower order of magnitude, these frequencies are not negligible. The frequencies should be at least three times the frequency that can be recorded for negligible contribution to the error. Although the gages used are mechanically overdamped so that no resonance effects are observed, the resonance frequencies determines the lower limit to the highest frequency of faithful response. The factor 3 used is an old rule of thumb which should be used with discretion.

CONCLUSION

Air shock gages for side-on pressure disturb the flow about the gages depending on their thickness ratios and position of measurement on the gage housings. Wind tunnel tests show that error is dependent upon the flow velocity and Reynolds number. The ranges of Reynolds numbers for the test were 2.8×10^6 per ft to 8.6×10^6 per ft and free stream pressures were from 0.29×10^{-2} atm to 0.58×10^{-2} atm. For air with shock flow velocities between Mach 0.802 and 2.183, the Reynolds numbers are 11.2×10^6 per ft to 64×10^6 per ft. The Reynolds numbers behind shock at sea level are much higher, hence conditions are not comparable. The tests do show that as Reynolds number decreases the error increases, which is what happens when measurements are made at reduced atmospheric conditions. Shock tube tests on a pancake gage at subsonic speeds also show error increasing with increasing Mach number and atmospheric condition.[18]

The gage thickness ratio should be less than 0.1 and the transducer should be positioned away from the leading edge. The shaft should not be thicker than the gage.

The error due to the angle of attack is small if the angle of attack is less than 1°. Gages in the form of a long glat plate with a circular arc-type leading edge are practical for pressure measurements as shown in Figure 6.[15-16]

The computed response and impulse of a transducer is dependent upon whether a pulse is terminated or not. The pulse should not be terminated when considering experimental response and impulse because of the large influence of the negative phase of the pulse.

The diaphragm frequencies should not be neglected when the gage is constructed; when piezoelectric elements such as Tourmaline are used, the diaphragm may be omitted.

ACKNOWLEDGMENTS

The experiments in the BRL Supersonic and Hypersonic Tunnel were conducted by Mr. Maurice Sylvester. This work is gratefully acknowledged.

The contribution of Mr. William Webster of Weapon Systems Laboratory, in checking the mathematics is also gratefully acknowledged.

HENRY J. GOODMAN

REFERENCES

1. MacDonald, J. K. L. and Schaaf, S. A. On the Estimation of Perturbation due to Flow Around Blast Gages. Applied Mathematics Note No. 22 (Applied Mathematics Group - New York University No. 136), September 1945.

2. Taylor, G. I. Pressures on Solid Bodies Near an Explosion. The Scientific Papers of G. I. Taylor, Volume III, Cambridge at the University Press, 1963.

3. Shear, Ralph E. and Day, B. D. Tables of Thermodynamic and Shock Front Parameters for Air. Ballistic Research Laboratories Memorandum Report No. 1206, May 1959.

4. Unpublished work of Mr. Ray Sedney, Ballistic Research Laboratories.

5. Willmarth, W. W. On the Measurement of Surface Pressure with a Static Probe. Journal of the Aeronautical Science, Volume 2V, p. 438, 1953.

6. Briggs, L. J. and Dreyden, H. L. Pressure Distribution Over Airfoils at High Speeds. Twelfth Annual Report of NACA, Report No. 255, 1926.

7. Liepmann, H. W.; Askenas, H. and Cole, J. D. Experiments in Transonic Flow. USAF Technical Report No. 5667, USAF Air Material Command, Wright-Patterson Air Force Base, Dayton, Ohio, 1948.

8. Askenas, Harry I and Bayson, Arthur E. Design and Performance of a Simple Interferometer for Wind Tunnel Measurement. Journal of the Aeronautical Science, Volume 18, p. 82, 1931.

9. Lindsey, Walter F. and Landrum, Emma Jean Compilation of Information on Transonic Attachment of Flows at the Leading Edges of Airfoils. NACA Technical Note No. 4204, Langley Aeronautical Laboratory, Langley Field, Virginia, 1958.

10. Curtis, Wesley. Air Blast Measurements on Spherical Pentolite. Ballistic Research Laboratories Memorandum Report No. 544, July 1951.

11. Fader, W. J. Effect of Gauge Size on the Measurement of Air Blast. Ballistic Research Laboratories Technical Note No. 551, September 1951.

12. Arons, A. B. and Cole, R. H. Design and Use of Piezoelectric Gages for Measurement of Large Transient Pressures. The Review of Scientific Instruments, Volume 21, No. 1, January 1958.

13. Arons, A. B. and Tait, C. W. Design and Use of Tourmaline Gauges for Piezoelectric Measurements of Air Blast. NDRC Report No. A372, Division 2, NDRC, Washington, D.C., 1946.

14. Hearst, J. R.; Irani, G. B. and Geesaman, L. B. Piezoelectric Response of Z-Cut Tourmaline to Shocks of up to 21 Kilobars. Journal of Applied Physics, Volume 36, No. 11, 1965.

15. Jefferys, R. C.; Berry, F. J. and Deas, P. J. The Measurement of Air Blast: A Theoretical Analysis of the Response of H3 Gauge to a Blast Wave. RARDE Memorandum (MX) 46/62, Materials Explosive Division, Fort Halstead, Kentucky, 1962.

16. Armstrong, A. H. and Hicks, E. P. The Aerodynamic Calibration of Blast Pressure Gauges. ARE Report No. 34/50, Physical Research Division, Fort Halstead, Kentucky, 1951.

17. Condon, E. V. and Odishaw, H. Handbook of Physics. McGraw-Hill Book Co., Inc., p. 3-109, 1958.

18. Ruetenik, J. Ray and Lewis, S. Dean Pressure Probe and System for Measuring Large Blast Wave. Technical Report No. AFDL-TDR-65-35, Wright-Patterson Air Force Base, Ohio, June 1965.

BLANK PAGE

Unclassified

Security Classification

DOCUMENT CONTROL DATA - R&D

(Security classification of title, body of abstract and indexing annotation must be entered when the overall report is classified)

1. ORIGINATING ACTIVITY (Corporate author)
U.S. Army Ballistic Research Laboratories
Aberdeen Proving Ground, Maryland

2a. REPORT SECURITY CLASSIFICATION
Unclassified

2b. GROUP

3. REPORT TITLE
AERODYNAMIC AND FREQUENCY DEPENDENT ERRORS IN AN AIR BLAST GAGE

4. DESCRIPTIVE NOTES (Type of report and inclusive dates)

5. AUTHOR(S) (Last name, first name, initial)
Goodman, Henry J.

6. REPORT DATE	7a. TOTAL NO. OF PAGES	7b. NO. OF REFS
October 1966	70	18

8a. CONTRACT OR GRANT NO.	9a. ORIGINATOR'S REPORT NUMBER(S)
b. PROJECT NO. RDT&E-1P014501A33E	Report No. 1345
c.	9b. OTHER REPORT NO(S) (Any other numbers that may be assigned this report)
d.	

10. AVAILABILITY/LIMITATION NOTICES
Distribution of this document is unlimited.

11. SUPPLEMENTARY NOTES	12. SPONSORING MILITARY ACTIVITY
	U.S. Army Materiel Command Washington, D.C.

13. ABSTRACT

Tests were conducted in the Ballistic Research Laboratories (BRL) supersonic and hypersonic wind tunnel to determine the aerodynamic error due to mass flow around a pancake type gage. This air blast gage has been used extensively to measure the transient side-on pressure generated by an explosive charge. Data on flat surfaces are also presented.

The error due to mass flow is a function of both Mach number and Reynolds number. Error is largest near Mach one.

Measurements of impulse on gages with various shapes of pulses are considered. If there is no negative phase, impulse is independent of the gage size; the negative phase results in a low value of impulse for a gage longer than 1/10 the length of the positive phase.

DD FORM 1 JAN 64 1473

Unclassified

Security Classification

14 KEY WORDS	LINK A		LINK B		LINK C	
	ROLE	WT	ROLE	WT	ROLE	WT
Explosive Air Blast Gage Side-On Pressure Measurement Error Air Blast Gage Response Aerodynamic Error						

INSTRUCTIONS

1. ORIGINATING ACTIVITY: Enter the name and address of the contractor, subcontractor, grantee, Department of Defense activity or other organization *(corporate author)* issuing the report.

2a. REPORT SECURITY CLASSIFICATION: Enter the overall security classification of the report. Indicate whether "Restricted Data" is included. Marking is to be in accordance with appropriate security regulations.

2b. GROUP: Automatic downgrading is specified in DoD Directive 5200.10 and Armed Forces Industrial Manual. Enter the group number. Also, when applicable, show that optional markings have been used for Group 3 and Group 4 as authorized.

3. REPORT TITLE: Enter the complete report title in all capital letters. Titles in all cases should be unclassified. If a meaningful title cannot be selected without classification, show title classification in all capitals in parenthesis immediately following the title.

4. DESCRIPTIVE NOTES: If appropriate, enter the type of report, e.g., interim, progress, summary, annual, or final. Give the inclusive dates when a specific reporting period is covered.

5. AUTHOR(S): Enter the name(s) of author(s) as shown on or in the report. Enter last name, first name, middle initial. If military, show rank and branch of service. The name of the principal author is an absolute minimum requirement.

6. REPORT DATE: Enter the date of the report as day, month, year; or month, year. If more than one date appears on the report, use date of publication.

7a. TOTAL NUMBER OF PAGES: The total page count should follow normal pagination procedures, i.e., enter the number of pages containing information.

7b. NUMBER OF REFERENCES: Enter the total number of references cited in the report.

8a. CONTRACT OR GRANT NUMBER: If appropriate, enter the applicable number of the contract or grant under which the report was written.

8b, 8c, & 8d. PROJECT NUMBER: Enter the appropriate military department identification, such as project number, subproject number, system numbers, task number, etc.

9a. ORIGINATOR'S REPORT NUMBER(S): Enter the official report number by which the document will be identified and controlled by the originating activity. This number must be unique to this report.

9b. OTHER REPORT NUMBER(S): If the report has been assigned any other report numbers *(either by the originator or by the sponsor)*, also enter this number(s).

10. AVAILABILITY/LIMITATION NOTICES: Enter any limitations on further dissemination of the report, other than those imposed by security classification, using standard statements such as:

(1) "Qualified requesters may obtain copies of this report from DDC."

(2) "Foreign announcement and dissemination of this report by DDC is not authorized."

(3) "U. S. Government agencies may obtain copies of this report directly from DDC. Other qualified DDC users shall request through _____."

(4) "U. S. military agencies may obtain copies of this report directly from DDC. Other qualified users shall request through _____."

(5) "All distribution of this report is controlled. Qualified DDC users shall request through _____."

If the report has been furnished to the Office of Technical Services, Department of Commerce, for sale to the public, indicate this fact and enter the price, if known.

11. SUPPLEMENTARY NOTES: Use for additional explanatory notes.

12. SPONSORING MILITARY ACTIVITY: Enter the name of the departmental project office or laboratory sponsoring *(paying for)* the research and development. Include address.

13. ABSTRACT: Enter an abstract giving a brief and factual summary of the document indicative of the report, even though it may also appear elsewhere in the body of the technical report. If additional space is required, a continuation sheet shall be attached.

It is highly desirable that the abstract of classified reports be unclassified. Each paragraph of the abstract shall end with an indication of the military security classification of the information in the paragraph, represented as *(TS)*, *(S)*, *(C)*, or *(U)*.

There is no limitation on the length of the abstract. However, the suggested length is from 150 to 225 words.

14. KEY WORDS: Key words are technically meaningful terms or short phrases that characterize a report and may be used as index entries for cataloging the report. Key words must be selected so that no security classification is required. Identifiers, such as equipment model designation, trade name, military project code name, geographic location, may be used as key words but will be followed by an indication of technical context. The assignment of links, rules, and weights is optional.